ER-resident transmembrane kinase, IRE1. IRE1 senses the perturbed environment in the ER lumen and leads the signaling downstream to induce ER-resident chaperones such as GRP78/BiP, which facilitate protein folding [14]. This process was suggested to depend on oligomerization and autophosphorylation of IRE1 [14]. A second arm of the UPR consists of the suppression of protein translation. It has been suggested that reduced protein synthesis rates during ER stress serve to reduce the load of substrates presented to the folding machinery in the ER lumen. This correlates with enhanced phosphorylation of the α subunit of eukaryotic translation initiation factor 2 (eIF2α) [15]. It was also reported that PKR-like ER kinase (PERK) participates in coupling ER stress to translation inhibition by phosphorylating eIF2α [16,17]. The luminal domain of this kinase is related in sequence to that of IRE1 [17], suggesting that these kinases are simultaneously activated by the accumulation of malfolded proteins. We previously reported that the PS1 mutations found in patients with FAD led to attenuation of the induction of GRP78/BiP under ER stress conditions by inhibiting the phosphorylation of IRE1 [18]. In the present study, to analyze further the mechanism by which mutant PS1 downregulates the ER stress response, we examined whether PS1 mutants affect the signaling pathways mediated by another ER stress transducer, PERK.

Materials and methods

Expression plasmid and transfection. Wild-type and ΔE9 PS1 cDNAs were cloned into pcDNA3 (Invitrogen) as described previously [18]. Mouse Neuro2a (N2a) cells were transfected with each expression plasmid using lipofectamine 2000 (Gibco), and each stable transformant was established by G418 (Wako) selection.

Culture of fibroblasts from PS1 mutant knock-in mice. Primary fibroblasts were cultured from PS1 mutant (I213T) knock-in embryos on embryonic day 14.5, generated by mating heterozygous knock-in mice as described [19]. These cells were grown in DMEM supplemented with 10% fetal calf serum and were treated with 0.5 mM dithiothreitol (DTT) (Sigma) for specified times.

Antibodies. Rabbit antisera against a synthetic peptide corresponding to residues 1–14 of human PS1 have been previously described [18]. Anti-PERK antibody was raised against a synthetic peptide corresponding to residues of PERK (residues 1094–1114) and was affinity-purified using Prot On Kit1 (Multiple Peptide System, San Diego) [20]. Anti-KDEL monoclonal antibody, anti-PS1 monoclonal antibody, and anti-phosphorylated eIF2α polyclonal antibodies were purchased from Stressgen, Chemicon, and Research Genetics Company, respectively.

Fluorescent microscopy. PS1-transfected N2a cells were fixed with 4% paraformaldehyde and permeabilized with 0.3% Triton X-100 for 10 min. The fixed cells were incubated with anti-PERK, anti-PS1, and/or anti-KDEL antibodies at dilutions of 1:500 for 5 h at 4 °C and were stained with FITC-conjugated anti-rabbit IgG (Gibco) or Cy3-conjugated anti-rat IgG (Gibco) antibodies for 2 h. The stained cells were observed using a confocal microscope (Axioplan 2; Carl Zeiss).

Induction of ER stress and Western blotting. For Western blotting of PERK, 3×10^5 N2a cells that were transfected with each PS1 construct were plated in 6-cm diameter dishes 2 days before the treatment with the ER stress inducer, 1 μM thapsigargin (Sigma). Sixty-percent confluent cultures were used to avoid various stresses induced by overgrowth and were placed in fresh media for more than 1 h before stress treatment with ER stressors. After being washed twice with ice-cold phosphate buffered saline (PBS), cells were lysed in 200 μl of Triton buffer (20 mM HEPES, pH 7.5, 150 mM NaCl, 1% Triton X-100, 10% glycerol, 1 mM EDTA, 10 mM tetrasodium pyrophosphate, 100 mM NaF, 17.5 mM β-glycerophosphate, 1 mM phenylmethylsulfonyl fluoride (PMSF), 4 mg/ml aprotinin, and 2 mg/ml pepstatin A). All samples were centrifuged for 10 min at 4 °C after being placed on ice for 1 h, and supernatants were collected. After the protein concentration of each sample was quantified using a bicinchoninic acid-based Protein Assay Kit (Pierce). Samples were loaded onto an SDS–polyacrylamide gel. Protein-equivalent samples were subjected to Western blotting. The ratio of phosphorylated PERK (P-PERK) signal to the total PERK signal and the intensity of the phosphorylated eIF2α (P-eIF2α) in each lane were quantified densitometrically.

Metabolic labeling. To measure translational inhibition, sixty-percent confluent 6-cm diameter dishes of PS1-transfected N2a cells were washed twice with PBS and placed in 1.5 ml of serum-free ES media (Gibco BRL) containing 3 mg/L L-methionine and 4.8 mg/L L-cysteine. Cells were then pretreated for 20 min with or without 400 nM thapsigargin. The cells were pulse labeled for 10 min with 50 μCi of [^{35}S]methionine/cysteine express labeling mix (ICN Biochemicals) in methionine/cysteine-free DMEM containing 10% dialyzed fetal bovine serum, washed twice with ice-cold PBS containing unlabeled L-methionine (0.6 mg/ml) and L-cysteine (0.96 mg/ml), and lysed in 300 μl of Triton buffer. The lysate was clarified by centrifugation, and 20 μl was separated by SDS–PAGE. The gels were fixed, dried, and exposed for autoradiography. The levels of protein synthesis were quantified in four experiments by densitometry of autoradiogram films. The levels of [^{35}S] incorporation into proteins in the untreated cells were normalized to 100%.

Results and discussion

Previously, we showed that FAD-linked PS1 mutants downregulate a signaling pathway of the UPR. This is caused by decreased levels of phosphorylated-IRE1, which activates transcription of molecular chaperones such as GRP78/BiP [18]. In the present study, we attempted to clarify whether the PS1 mutants influence the activation of PERK, another ER stress transducer, under ER stress conditions. The luminal domain of PERK is similar in sequence to that of IRE1 [18,21,22]. We established mouse N2a cells stably expressing wild-type PS1 or PS1 with an exon 9 deletion (ΔE9) [23].

To investigate whether mutant PS1 (ΔE9) influenced on the localization of PERK, we studied the subcellular localization of PS1 and PERK in N2a cells stably expressing wild-type PS1 and ΔE9. Immunofluorescence microscopy showed that PS1 is preferentially distributed in the ER, Golgi, and cytoplasmic membrane, as described previously [24,25]. PERK was localized to the ER, as shown by the exclusive colocalization of PERK immunoreactivity with GRP78/BiP and GRP94, which are resident in the ER as detected by anti-KDEL antibody. Double labeling showed that in N2a cells overexpressing wild-type PS1, the immunoreactivity overlapped with that of PERK in the ER (data not

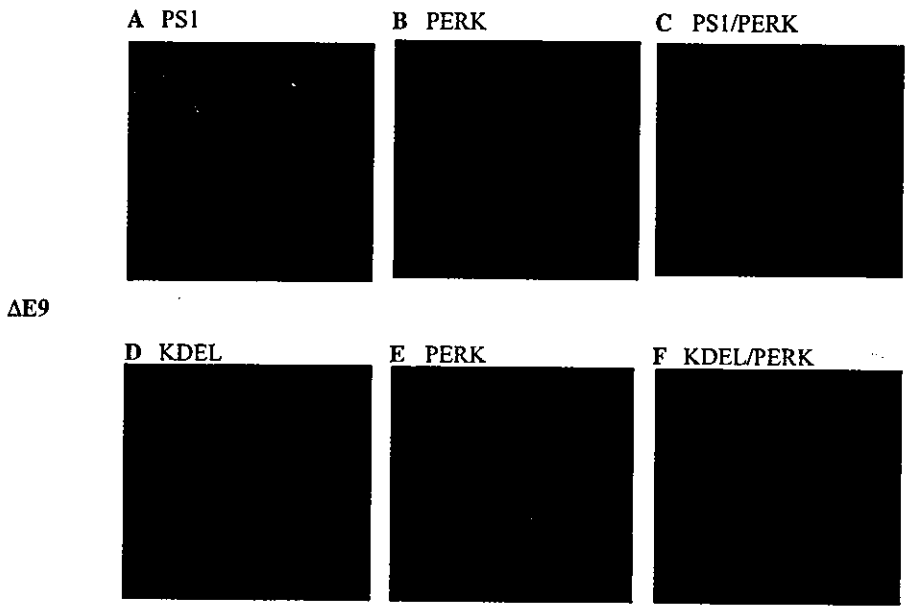

Fig. 1. Localization of PS1 in N2a cells with Δ exon 9 mutant PS1 (ΔE9) overlapped with that of the ER stress sensor PERK or GRP78/BiP, same as the cell with wild-type PS1. Immunostaining for PS1/PERK in the N2a cells. (A, PS1, red; B, PERK, green; C, overlapping, yellow.) D–F, Immunostaining for PS1/KDEL in the N2a cells. (D, PERK, green; E, KDEL, red; F, overlapping, yellow.) Anti-KDEL antibody detects both GRP78/BiP and GRP94 (as ER markers).

shown). A similar distribution was observed in the cells expressing the mutant PS1, ΔE9 (Fig. 1), indicating that mutant PS1 does not alter the distribution of PERK in the ER.

We examined the response of PERK-eIF2α signaling-pathway by ER stress in the N2a cells stably expressing mock, wild-type PS1, and ΔE9. Before treatments with ER stressors, we pre-treated the cells with fresh medium

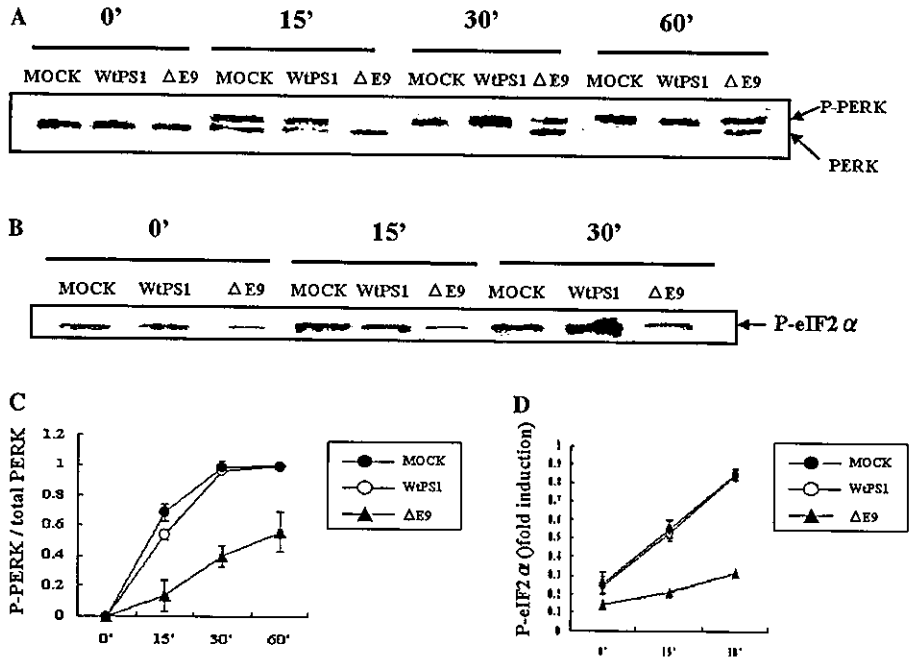

Fig. 2. PS1 mutant, ΔE9, inhibits the activation of PERK and its downstream signal eIF2α in N2a cells. Cells were stably transfected with each PS1 construct (MOCK, empty vector; wtPS1, wild-type PS1; ΔE9, Δ exon 9 mutant PS1). The cells were treated for the indicated periods of time with an agent that promotes ER stress, 1 μM thapsigargin (Tg), after pretreatment. The cells were lysed in Triton buffer followed by Western blotting. (A) The blot was incubated with an antibody that detects both non-phosphorylated (inactive) PERK and the phosphorylated (activated) form of the protein (P-PERK). (B) The blot was incubated with an antibody specific to eIF2α phosphorylated on serine 51 (P-eIF2α). (C) The ratio of phosphorylated PERK (P-PERK) to the total PERK signal of each lane in (A) was quantified densitometrically ($n = 4$; means ± SEM). (D) Fold inductions of phosphorylated eIF2α (P-eIF2α) of each lane in (B) was quantified densitometrically ($n = 4$; means ± SEM).

for more than 1 h to obtain baseline data. After pre-incubation, the cells were exposed to 1 μM thapsigargin, an inhibitor of the sarco-endoplasmic reticulum Ca^{2+}-ATPase (SERCA) pump (Fig. 2). Stress-induced activation of the protein kinase PERK stimulates phosphorylation PERK itself, which can be evaluated by a mobility shift of the PERK band upon SDS–PAGE [14], and the ratio of phosphorylated PERK (P-PERK) to the total PERK of each lane was analyzed densitometrically. Basal expression levels of PERK were not altered in N2a cell lines stably expressing each construct (Fig. 2A). In N2a cells transfected with empty vector (MOCK) or wild-type PS1, PERK completely underwent a shift in its mobility within 30 min after treatment with thapsigargin (Figs. 2A and C), suggesting that PERK was predominantly phosphorylated by the ER stressor in the cells with MOCK and wild-type PS1. In contrast, in cells expressing the PS1 mutant, ΔE9, PERK was only partially phosphorylated, even 30 min after thapsigargin treatment (Figs. 2A and C). Furthermore, since PERK is an ER-resident transmembrane protein kinase that phosphorylates eIF2α to downregulate protein synthesis under ER stress. Therefore, we examined the levels of phosphorylated-eIF2α of the same lysates from N2a cells, quantifying these levels densitometrically. As was expected, in PS1 mutant-expressing cells, phosphorylation of eIF2α was not complete within 15 min, whereas the phosphorylation occurred almost more immediately in cells with MOCK and wild-type PS1 than in mutant PS1 (Fig. 2B and D). We attempted the same experiments as described in Fig. 2 with another ER stress-inducing agent, DTT (1 mM), a reversible inhibitor of protein folding in the ER. The mutant PS1-expressing cells also retarded both the phosphorylation of PERK and the phosphorylation of eIF2α by DTT (data not shown). These findings indicated that the PS1 mutation impairs the activation of PERK and subsequently inhibits the phosphorylation of eIF2α.

To exclude the possibility that these phenomena were caused by overexpression of the PS1 mutation or that they were due to the unique mutation of PS1, ΔE9, we studied primary cultured fibroblasts derived from embryos of PS1 mutant 'knock-in' mice that express mutant PS1 (I213T) [19]. Without ER stress, the total amount of PERK in fibroblasts from homozygous knock-in mice were similar in fibroblasts from the wild-type mice (Fig. 3). When we treated them with 0.5 mM DTT, the phosphorylation of PERK was disturbed in primary cultured fibroblasts from PS1 homozygous knock-in mice in comparison with that in fibroblasts from their wild-type littermates (Fig. 3). These results were completely consistent with those observed in the N2a cell lines. It is, therefore, clear that the mutations in PS1, not only ΔE9, attenuate the activation of PERK under ER stress regardless of its expression level.

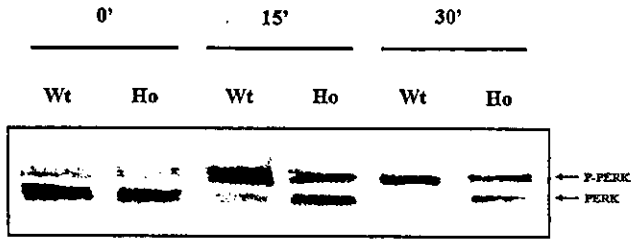

Fig. 3. Phosphorylation of PERK was impaired in primary cultured fibroblasts derived from PS1 mutant knock-in mice. Primary cultured fibroblasts from PS1 mutation (I213T) knock-in mice were treated with 0.5 mM dithiothreitol (DTT), which promotes ER stress, for the indicated periods after pretreatment. The cells were lysed in Triton buffer followed by Western blotting. The phosphorylation of PERK was disturbed in primary cultured fibroblasts from PS1 homozygous knock-in mice in comparison with that in fibroblasts from their wild-type littermates within 15 min of DTT treatment. (Wt, wild-type; Ho, homozygous mutant (I213T); P-PERK; phosphorylated PERK.)

The outcome of stimulation of the PERK-eIF2α pathway is the attenuation of translation. We further confirmed whether the FAD-linked PS1 mutation actually influenced the regulation of translation when treated with agents that induce ER stress. N2a cells containing wild-type PS1 or mutant PS1 were cultured with or without 400 nM thapsigargin for 20 min and pulse-labeled for 10 min with [^{35}S]methionine/cysteine. N2a cells containing wild-type PS1 exhibited a profound attenuation in global translation rate. This is reflected in the reduced incorporation of [^{35}S]methionine/cysteine into cellular proteins following a short labeling pulse in the presence of ER stress-inducing agents. In contrast, the cells containing mutant PS1 did not reduce their translation rate when exposed to thapsigargin (Fig. 4). A recent study showed that *Perk*$^{-/-}$ cells have impaired attenuation of protein synthesis under ER stress and

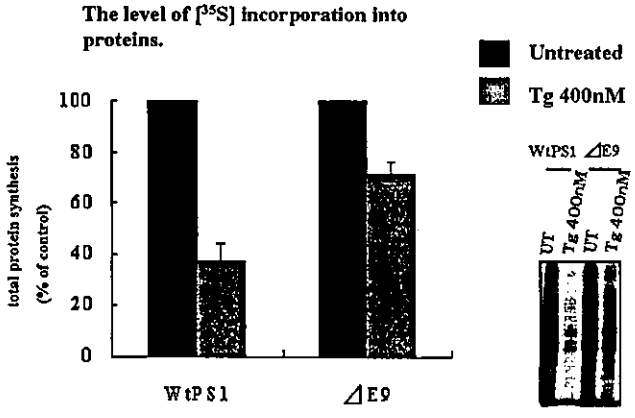

Fig. 4. Protein synthesis rates were studied by the incorporation of [^{35}S]methionine/cysteine into proteins during 10 min of pulse labeling that is followed by 20 min of exposure to thapsigargin (400 nM). Total protein synthesis level in 30 min was more suppressed in the cells with wild-type PS1 than ΔE9. The levels of protein synthesis were quantified by densitometry of autoradiograms. The level of [^{35}S] incorporation into proteins in the untreated cells was normalized to 100% ($n = 4$; means ± SEM). The inset shows the representative autograms.

that PERK is essential to translational regulation and cell survival during the UPR [22]. Our results showed that mutant PS1 disturbs the regulation of protein synthesis levels through the signaling pathway of PERK and eIF2α and may result in impediment of cell survival.

However, it remains unclear how mutant PS1 inhibits the activation of ER stress transducers. Recently, it was proposed that activation of the ER stress transducers could be triggered by dissociation of GRP78/BiP from the stress transducers per se [14]. The dissociation leads to oligomerization of stress transducers inducing its autophosphorylation and then activation of downstream signaling. If PS1 mutants form malfolded structures, GRP78/BiP may inevitably bind to PS1 molecules to promote their folding. The formation of a complex of mutant PS1, PERK (or IRE1), and GRP78/BiP may inhibit the dissociation of GRP78/BiP from PERK or IRE1 under ER stress.

It is possible that PERK may associate with mutant PS1 as well as wild-type PS1 in the ER. However, it is unknown whether mutant PS1, which may be malfolded in the ER, associates with GRP78/BiP. Further study is needed to examine whether mutant PS1 inhibits the dissociation of GRP78/BiP from PERK during ER stress to clarify the mechanisms responsible for disturbed function of PERK by PS1 mutation.

In the brains of patients with Alzheimer's disease, Aβ deposition is one of important pathologic features. FAD-linked PS1 mutants alter the processing of APP and increased the production of the more amyloidogenic Aβ peptide, Aβ42 [6,7]. Therefore, whether the attenuation of the UPR causes the production of Aβ42 should be clarified. It has been reported that ER stress activates retrograde transport from the Golgi to the ER to prevent malfolded proteins from moving to targeted organelles [26]. Because the distribution of APP and its secretase affect the generation of Aβ42 [27], prolonged ER stress may shift their distribution to the ER and may change Aβ production. Our current study showed that the PERK-eIF2α pathway, as well as the IRE-GRP78/Bip pathway, is attenuated in cells with PS1 mutations. The disturbed UPR may prolong ER stress. These conditions may change Aβ production and lead cells to apoptosis. It is uncertain whether disturbed UPR, which prolongs ER stress, accelerates Aβ production. We are therefore currently analyzing Aβ production in PERK knockout cells, whose UPR is attenuated under ER stress.

In conclusion, our findings suggest that the attenuation of the UPR by a PS1 mutations may be one of the pathologic processes in FAD.

Acknowledgment

This work was financially supported in part by the Gotoda foundation.

References

[1] E.I. Rogaev, R. Sherrington, E.A. Rogaeva, G. Levesque, et al., Familial Alzheimer's disease in kinders with missense mutations in a gene on chromosome 1 related to the Alzheimer's disease type 3 gene, Nature 376 (1995) 775–778.
[2] R. Sherrington, E.I. Rogaev, Y. Liang, E.A. Rogaeva, G. Levesque, et al., Cloning of a gene bearing missense mutations in early-onset familial Alzheimer's disease, Nature 375 (1995) 754–760.
[3] P.H.St. George-Hyslop, J. Haines, E. Rogaev, M. Mortilla, G. Vaula, et al., Genetic evidence for a novel familial Alzheimer's disease locus on chromosome 14, Nat. Genet. 2 (1992) 330–334.
[4] E. Levy-Lahad, E.M. Wijsman, E. Nemens, L. Anderson, et al., A familial Alzheimer's disease locus on chromosome 1, Science 269 (1995) 970–973.
[5] E. Levy-Lahad, W. Wasco, P.D.M. Poorkaj, et al., Candidate gene for the chromosome 1 familial Alzheimer's disease locus, Science 269 (1995) 973–977.
[6] D.R. Borchelt, G. Thinakaran, C.B. Eckman, et al., Familial Alzheimer's disease-linked presenilin 1 variants elevate Aβ1–42/1–40 ratio in vitro and in vivo, Neuron 17 (1996) 1005–1013.
[7] C. Duff, K. Eckman, C. Zehr, et al., Increased amyloid-β42(43) in brains of mice expressing mutant presenilin 1, Nature 24 (1996) 710–713.
[8] J. Walter, A. Capell, J. Grunberg, et al., The Alzheimer's disease-associated presenilins are differentially phosphorylated proteins located predominantly within the endoplasmic reticulum, Mol. Med. 2 (1996) 673–691.
[9] J.G. Culvenor, F. Maher, G. Evin, et al., Alzheimer's disease-associated presenilin 1 in neuronal cells: evidence for localization to the endoplasmic reticulum-Golgi intermediate compartment, J. Neurosci. Res. 49 (1997) 719–731.
[10] W.G. Annaert, L. Levesque, K. Craessaerts, et al., Presenilin 1 controls γ-secretase processing of amyloid precursor protein in pre-golgi compartments of hippocampal neurons, J. Cell Biol. 147 (1999) 277–294.
[11] R.J. Kaufman, Stress signaling from the lumen of the endoplasmic reticulum: coordination of gene transcriptional and translational controls, Genes Dev. 13 (1999) 1211–1233.
[12] K. Mori, Tripartite management of unfolded proteins in the endoplasmic reticulum, Cell 101 (2000) 451–454.
[13] C.O. Brostrom, M.A. Brostrom, Regulation of translational initiation during cellular responses to stress, Prog. Nucleic Acid Res. Mol. Biol. 58 (1998) 79–125.
[14] A. Bertolotti, Y. Zang, L.M. Hendershot, H.P. Harding, D. Ron, Dynamic interaction of BiP and ER stress transducers in the unfolded protein response, Nat. Cell. Biol. 2 (2000) 326–332.
[15] Y. Shi et al., Identification and characterization of pancreatic eukaryotic initiation factor 2 α-subunit kinase, PEK, involved in translational control, Mol. Cell Biol. 18 (1998) 7499–7509.
[16] C.R. Prostko, M.A. Brostrom, C.O. Brostrom, Reversible phosphorylation of eukaryotic initiation factor 2α in response to endoplasmic reticular signaling, Mol. Cell. Biochem. 127–128 (1993) 255–256.
[17] H.P. Harding, Y. Zhang, D. Ron, Protein translation and folding are coupled by an endoplasmic-reticulum-resident kinase, Nature 397 (1999) 21.
[18] T. Katayama, K. Imaizumi, N. Sato, K. Miyoshi, T. Kudo, et al., Presenilin-1 mutations downregulate the signaling pathway of the unfolded protein response, Nat. Cell. Biol. 1 (1999) 479–485.
[19] Y. Nakano, G. Kondoh, T. Kudo, K. Imaizumi, M. Kato, J.I. Miyazaki, M. Tohyama, J. Takeda, M. Takeda, Accumulation of murine amyloid β42 with a gene-dosage dependent manner in PS1'knock-in' mice, Eur. J. Neurosci. 11 (1999) 2577–2581.
[20] T. Katayama, K. Imaizumi, A. Honda, T. Yoneda, T. Kudo, et al., Disturbed activation of endoplasmic reticulum stress transducers

by familial Alzheimer's disease-linked presenilin-1 mutations, J. Biol. Chem. 16 (2001) 43446–43454.
[21] H.P. Harding, I. Novoa, Y. Zhang, H. Zeng, M. Schapira, D. Ron, Regulated translation initiation controls stress-induced gene expression in mammalian cells, Mol. Cell. 6 (2000) 1099–1108.
[22] H.P. Harding, Y. Zhang, A. Bertolotti, H. Zeng, D. Ron, PERK is essential for translational regulation and cell survival during the unfolded protein response, Mol. Cell. 5 (2000) 897–904.
[23] J.P. Tur, S. Froelich, G. Prihar, R. Crook, M. Baker, et al., A mutation in Alzheimer's disease destroying a splice acceptor site in the presenilin-1 gene, Neuroreport 7 (1995) 297–301.
[24] Q. Guo, B.L. Sopher, K. Furukawa, D.G. Pham, N. Robinson, et al., Alzheimer's Presenilin mutation sensitizes neural cells to apoptosis induced by trophic factor withdrawal and amyloid β-peptide: involvement of calcium and oxyradicals, J. Neurosci. 1 (1997) 4212–4222.
[25] Nazneen, N. Dewji, S.J. Singer, The seven-transmembrane spanning topography of Alzheimer's disease-related presenilin proteins in the plasma membranes of cultured cells, Proc. Natl. Acad. Sci. USA 94 (1997) 14025–14030.
[26] C. Hammond, A. Helenius, Quality control in the secretory pathway: retention of a misfolded viral membrane glycoprotein involves cycling between the ER, intermediate compartment, and Golgi apparatus, J. Cell Biol. 126 (1994) 41–52.
[27] D.G. Cook, M.S. Forman, J.C. Sung, S. Leight, D.L. Kolson, T.I. Watsubo, V.M. Lee, R.W. Doms, Alzheimer's Aβ(1–42) is generated in the endoplasmic reticulum/intermediate compartment of NT2N cells, Nat. Med. 3 (1997) 1021–1023.

The EMBO Journal Vol. 21 No. 20 pp. 5408–5416, 2002

Presenilins mediate a dual intramembranous γ-secretase cleavage of Notch-1

Masayasu Okochi, Harald Steiner[1], Akio Fukumori, Hisashi Tanii, Taisuke Tomita[2], Toshihisa Tanaka, Takeshi Iwatsubo[2], Takashi Kudo, Masatoshi Takeda[3] and Christian Haass[1]

Department of Post-Genomics and Diseases, Division of Psychiatry and Behavioral Proteomics, Osaka University Graduate School of Medicine, 565-0871 Osaka, [2]Department of Neuropathology and Neuroscience, Graduate School of Pharmaceutical Sciences, University of Tokyo, 113-0033 Tokyo, Japan and [1]Adolf-Butenandt-Institute, Department of Biochemistry, Laboratory for Alzheimer's and Parkinson's Disease Research, Ludwig-Maximilians-University, D-80336 Munich, Germany

[3]Corresponding author
e-mail: mtakeda@psy.med.osaka-u.ac.jp

Following ectodomain shedding, Notch-1 undergoes presenilin (PS)-dependent constitutive intramembranous endoproteolysis at site-3. This cleavage is similar to the PS-dependent γ-secretase cleavage of the β-amyloid precursor protein (βAPP). However, topological differences in cleavage resulting in amyloid β-peptide (Aβ) or the Notch-1 intracellular domain (NICD) indicated independent mechanisms of proteolytic cleavage. We now demonstrate the secretion of an N-terminal Notch-1 Aβ-like fragment (Nβ). Analysis of Nβ by MALDI-TOF MS revealed that Nβ is cleaved at a novel site (site-4, S4) near the middle of the transmembrane domain. Like the corresponding cleavage of βAPP at position 40 and 42 of the Aβ domain, S4 cleavage is PS dependent. The precision of this cleavage is affected by familial Alzheimer's disease-associated PS1 mutations similar to the pathological endoproteolysis of βAPP. Considering these similarities between intramembranous processing of Notch and βAPP, we conclude that these proteins are cleaved by a common mechanism utilizing the same protease, i.e. PS/γ-secretase.

Keywords: Notch signaling/Notch-1-β peptide/presenilin/γ-secretase/site-4 cleavage

Introduction

The Notch cell surface receptors are type I transmembrane domain (TM) proteins that are critically required for a variety of signaling events during embryogenesis and in adulthood (reviewed in Mumm and Kopan, 2000). Notch receptors undergo a cascade of endoproteolytic cleavages required for Notch signaling (reviewed in Mumm and Kopan, 2000). Upon binding of membrane-anchored ligands from the DSL (Delta/Serrate/Lag-2) family, Notch receptors undergo consecutive cleavages at site-2 (S2) and site-3 (S3) (reviewed in Mumm and Kopan, 2000). Cleavage of mouse Notch-1 at S2 occurs in its ectodomain by TACE [tumor necrosis factor-α (TNF-α)-converting enzyme], a member of the ADAM (a disintegrin and metalloprotease domain) family ~12 amino acids distant from the TM. This 'ectodomain shedding' event results in the generation of NEXT (Notch extracellular truncation; Brou *et al.*, 2000; Mumm *et al.*, 2000), that is cleaved subsequently at S3 within the TM close to the cytoplasmic border (Schroeter *et al.*, 1998). Cleavage of Notch at S3 liberates NICD (Notch intracellular domain) that translocates to the nucleus, where it is involved in target gene transcription (reviewed in Mumm and Kopan, 2000). S3 cleavage strictly depends on the biological activity of the presenilin (PS) proteins (reviewed in Steiner and Haass, 2000), which may contribute the catalytic site of γ-secretase, an unusual intramembrane-cleaving aspartyl protease complex (Wolfe *et al.*, 1999; Li *et al.*, 2000; Steiner *et al.*, 2000; Esler *et al.*, 2002a).

Beside the Notch-1–4 receptors (De Strooper *et al.*, 1999; Mizutani *et al.*, 2001; Saxena *et al.*, 2001), several other type I TM proteins have been identified as substrates for PS-dependent endoproteolysis, including the Alzheimer's disease (AD)-associated β-amyloid protein precursor (βAPP) (De Strooper *et al.*, 1998), ErbB-4 (Ni *et al.*, 2001; Lee *et al.*, 2002), E-cadherin (Marambaud *et al.*, 2002) and LRP (May *et al.*, 2002). These proteins undergo 'ectodomain shedding' in their large extracellular domains, prior to the consecutive PS-dependent cleavage within the TM. In the case of βAPP, these cleavages are mediated by α-secretase and β-secretase (reviewed in Esler and Wolfe, 2001). Cleavage of βAPP by α- and β-secretase (BACE) results in the generation of the respective βAPP C-terminal fragments (CTFs), CTFα and CTFβ, which are the direct substrates for γ-secretase cleavage. Cleavage of CTFβ and CTFα by γ-secretase occurs in the middle of the TM and leads to the liberation of Aβ and p3 peptides (Haass and Selkoe, 1993), respectively. Aβ is deposited in the brain of AD patients in 'senile plaques', an invariant pathological hallmark of AD (reviewed in Selkoe, 2001). Recently, the elusive C-terminal cleavage product of γ-secretase, AICD (βAPP intracellular domain), has been identified and characterized. Surprisingly, AICD results from PS-dependent γ-secretase cleavage of βAPP-CTFs predominantly after Leu49 (Aβ numbering). This cleavage is almost identical to the S3 cleavage of Notch-1 (Gu *et al.*, 2001; Sastre *et al.*, 2001; Yu *et al.*, 2001; Weidemann *et al.*, 2002) and does not occur after Val40 and Ala42 (Aβ numbering) as predicted. Thus, γ-secretase cleaves the βAPP TM at several sites: one in the middle after position 40 (γ_{40}) and 42 (γ_{42}) (with major γ_{40} and minor γ_{42} cleavage) and one close to the cytoplasmic border after position 49 (γ_{49}) of the Aβ domain. Interestingly, AICD may translocate to the nucleus where it could have a role in transcriptional

regulation (Cao and Südhof, 2001; Cupers *et al.*, 2001; Kimberly *et al.*, 2001; Gao and Pimplikar, 2002) similar to NICD.

Because of these striking similarities between Notch and βAPP endoproteolysis, we hypothesized that an Aβ/p3-like species (called Notch β-peptide, Nβ) derived from NEXT intramembranous proteolysis may be secreted into the extracellular space. Here we report the identification and characterization of secreted Nβ peptides derived from endoproteolysis of NEXT derivatives. Sequence analysis revealed that Nβ is derived from endoproteolytic cleavage near the middle of the Notch-1 TM at site-4 (S4), which is 12 amino acid residues upstream of S3. Like S3 cleavage, S4 cleavage occurs in a PS- and γ-secretase-dependent manner. Strikingly, familial AD (FAD)-associated PS mutants known to cause the increased production of C-terminally elongated pathogenic $A\beta_{42}$ also affect the generation of C-terminally elongated Nβ variants, supporting a direct role for PS in the proteolytic cleavage of Notch-1 and βAPP.

Results

Detection of a secreted Notch-1 Aβ-like peptide

Given the similarities between the endoproteolytic processing of βAPP and Notch, we hypothesized that Aβ-like peptides derived from an S2-cleaved membrane-retained NEXT fragment might be secreted into the extracellular space. In order to investigate this, we stably transfected human embryonic kidney 293 (K293) cells with F-NEXT, an N-terminally FLAG-tagged NΔE variant (Figure 1A). We first investigated whether F-NEXT undergoes constitutive S3 endoproteolysis like the well-characterized NΔE variant (Kopan *et al.*, 1996). F-NEXT- and NΔE-expressing cells were pulse labeled with [^{35}S]methionine for 1 h and chased for 2 h. Immunoprecipitation with anti-myc antibody 9E10 revealed robust amounts of F-NEXT and NΔE (Figure 1B). NICD was produced during the pulse labeling and the chase period and accumulated after 2 h of chase (Figure 1B), consistent with previous results (Steiner *et al.*, 1999a). To analyze secretion of Notch-1 peptides, the corresponding conditioned media were immunoprecipitated with the anti-FLAG antibody M2. Strikingly, robust amounts of a peptide of a molecular mass of ~4 kDa were observed in the conditioned media of F-NEXT-expressing cells after a 2 h chase period (Figure 1B). This peptide is secreted in a time-dependent manner (Figure 1C) similar to Aβ (Haass *et al.*, 1993) and did not accumulate inside the cells (Figure 1C). As expected, no M2-precipitable peptides were detected in the corresponding media of NΔE-expressing cells, demonstrating the specificity of the isolation procedure (Figure 1B). Untagged NΔE was also processed into a secreted peptide (data not shown). We conclude from these data that NEXT undergoes constitutive endoproteolysis resulting in the secretion of a peptide, which we term Notch-1-β peptide (Nβ) in analogy to Aβ.

Nβ is derived from intramembranous proteolysis at a novel cleavage site

We hypothesized that Notch-1 may undergo a γ_{40} analogous cleavage further N-terminal of S3, which could result in Nβ secretion. To determine the exact cleavage site of F-NEXT, we performed matrix-associated laser desorption ionization-time of flight mass spectrometry (MALDI-TOF MS) analysis of the secreted FLAG-tagged Nβ (F-Nβ). MALDI-TOF MS analysis of M2-immunoprecipitated F-Nβ revealed a major peak of a molecular mass of 3832 Da among several minor peaks, indicating heterogeneous processing of the Notch-1 TM (Figure 2A, inset; see Table I for the F-Nβ peptides identified in this study). Interestingly, the heterogeneity of the F-Nβ C-termini (see Table I) is similar to the C-terminal heterogeneity observed in secreted Aβ species (Wang *et al.*, 1996). Strikingly, the major F-Nβ peak corresponded to a peptide ending with Ala1731 (mouse Notch-1 numbering, Figure 2), indicating that F-Nβ is derived by a predominant cleavage at a novel site between Ala1731 and Ala1732, and not by cleavage at S3 between Gly1743 and Val1744 as predicted. This is consistent with the lack of any detectable F-Nβ species with a C-terminus corresponding to Gly1743 (see asterisk in Figure 2A). Identical results were obtained when Neuro2a, COS or CHO cells were used in this analysis (data not shown). Thus, these data strongly suggest that Notch-1, like βAPP, undergoes several distinct intramembranous cleavages: one close to the cytoplasmic border (S3) of the TM and a novel heterogeneous cut near the middle of the TM, which we now term site-4 (S4) cleavage (Figure 2B).

S4 cleavage is PS/γ-secretase dependent

Since $\gamma_{40/42}$ cleavage of βAPP has been shown to require PS activity (reviewed in Steiner and Haass, 2000), we next investigated whether S4 cleavage is also PS dependent. K293 cells expressing biologically inactive PS1 D385N (Steiner *et al.*, 1999b), which lacks one of the two putative active site aspartates (Wolfe *et al.*, 1999), were stably transfected with F-NEXT and analyzed for the generation of F-Nβ. Strikingly, F-Nβ generation was almost completely inhibited in cells expressing PS1 D385N (Figure 3A, upper panel). Consistent with previous results (Capell *et al.*, 2000), NICD production was also significantly reduced (Figure 3A, lower panel). To confirm further the PS/γ-secretase dependence of F-Nβ generation, we treated cells with the γ-secretase inhibitor L-685,458 (Shearman *et al.*, 2000). When L-685,458 was added to the pulse–chase experiment, an almost complete inhibition of F-Nβ generation was observed (Figure 3B, upper panel). As expected, NICD generation (Martys-Zage *et al.*, 2000; Beher *et al.*, 2001) was also blocked (Figure 3B, lower panel). Taken together, these results demonstrate that F-Nβ generation occurs by cleavage at S4 in a PS/γ-secretase-dependent manner similar to the generation of Aβ.

FAD-associated PS mutations affect S4 cleavage

All FAD-associated PS mutations analyzed so far result in the increased secretion of Aβ42 (reviewed in Steiner and Haass, 2000). We therefore investigated whether the PS-dependent S4 cleavage is also influenced by FAD-associated PS mutants. F-NEXT was stably transfected into K293 cells expressing wild-type PS1 or the FAD-associated PS1 mutants PS1 C92S, PS1 L166P and PS1 L286V (Kulic *et al.*, 2000; Okochi *et al.*, 2000; Moehlmann *et al.*, 2002). In particular, the L166P mutation was chosen because it not only causes one of

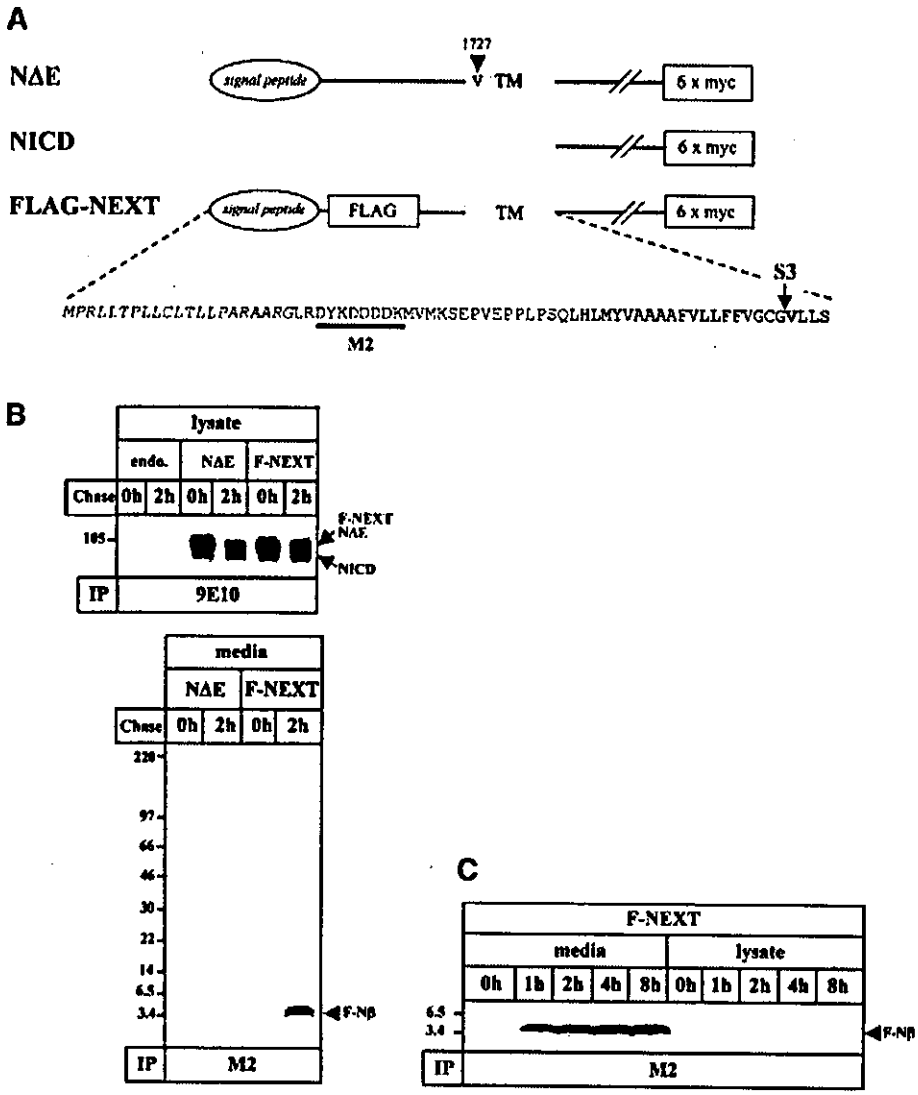

Fig. 1. Detection of a secreted Notch-1 fragment. (A) Schematic representation of NΔE, NICD and F-NEXT. All three mouse Notch-1 variants contain a hexametric myc tag at the C-terminus to facilitate detection. F-NEXT is a NΔE variant that contains an insertion of the FLAG epitope and two adjacent methionine residues after the signal peptide sequence to facilitate the detection of secreted Notch-1 fragments. An arrowhead indicates the M1727V mutation present in NΔE (Kopan *et al.*, 1996). An arrow shows S3, and the critical valine is shown in bold. The recognition site of the anti-FLAG antibody M2 is represented by the black bar. (B) Detection of a secreted FLAG-tagged Notch-1 fragment (F-Nβ) derived from F-NEXT. Untransfected K293 cells or K293 cells stably expressing NΔE or F-NEXT were pulse labeled with [^{35}S]methionine for 1 h and chased for 0 and 2 h. Upper panel: cell lysates were immunoprecipitated with anti-myc antibody 9E10. F-NEXT and NΔE undergo S3 cleavage with similar efficiency. Note that in this pulse–chase paradigm, NICD generation is detectable after pulse labeling for 1 h without chase. Lower panel: conditioned media from K293 cells stably expressing NΔE or F-NEXT were immunoprecipitated with anti-FLAG M2 agarose. (C) Time-dependent secretion of F-Nβ. K293 cells stably expressing F-NEXT were pulse labeled with [^{35}S]methionine for 1 h and chased for the indicated times. F-Nβ was analyzed in conditioned media, and cell lysates by immunoprecipitation with anti-FLAG M2 agarose. A longer exposure revealed that very low amounts of F-Nβ were also detectable in the cell lysates (data not shown). Identical results were obtained with F-NEXT M1727V (data not shown).

the strongest increases in Aβ42 generation, but also significantly inhibits S3 cleavage (Moehlmann *et al.*, 2002). Thus, this mutation allows investigation of whether a PS mutant that inhibits S3 cleavage also affects S4 cleavage. We analyzed the conditioned media of cells co-expressing the PS1 derivatives and F-NEXT by MALDI-TOF MS for putative alterations in the C-termini of F-Nβ. Strikingly, this revealed significant changes in the C-terminal cleavage pattern of Nβ produced in cells expressing wild-type or FAD mutant PS1 (Figure 4A). Specifically, the PS1 L166P mutation, which causes an extremely strong increase of Aβ42 generation (Moehlmann *et al.*, 2002), also produced strongly increased levels of elongated F-Nβ peptides. These include F-Nβ species elongated by two and four amino acids (F-Nβ1733 and F-Nβ1735; Figure 4B). In addition, levels of F-Nβ terminating at amino acid 1734 (Figure 4B) were also slightly but reproducibly elevated (Figure 4A). Thus, inhibition of S3 cleavage by the PS1 L166P mutant does not cause a block of S4 cleavage, but rather shifts the

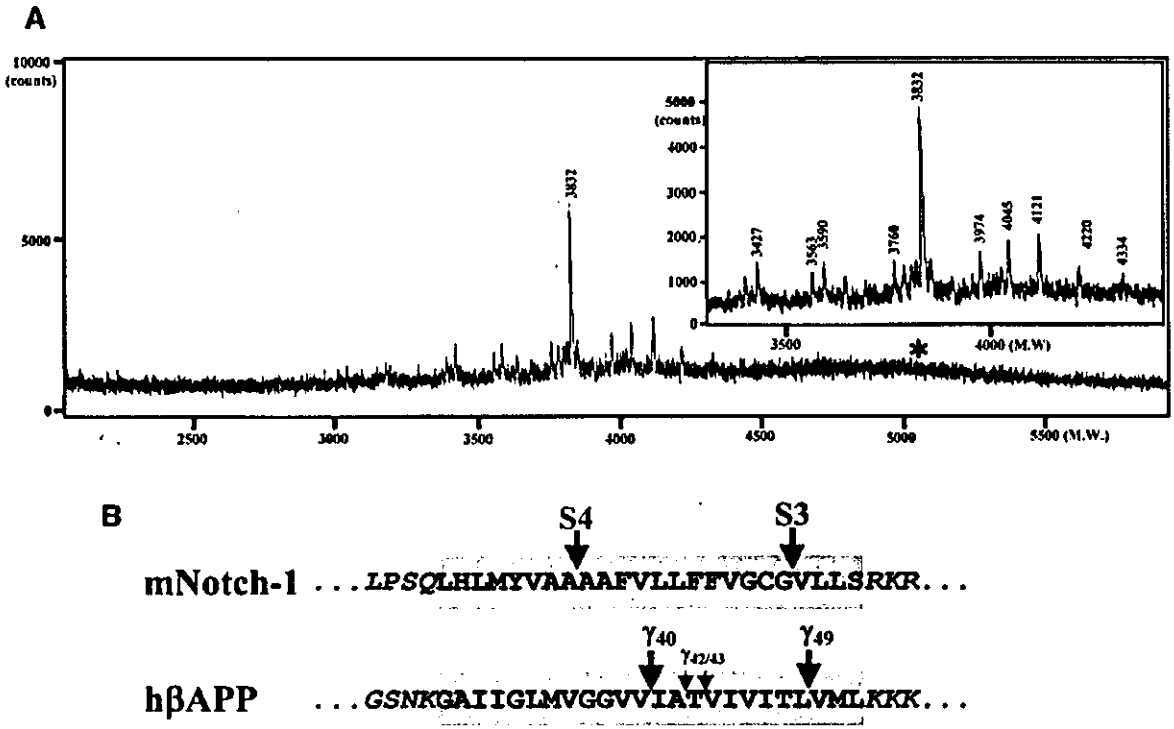

Fig. 2. Characterization of F-Nβ by IP/MS. (A) MALDI-TOF MS spectrum of F-Nβ. Conditioned medium from K293 cells stably expressing F-NEXT was immunoprecipitated with anti-FLAG M2 agarose, and F-Nβ was analyzed by MALDI-TOF MS (see Materials and methods). Molecular masses in Daltons of the individual peaks are indicated. Multiple peaks including a major peak at 3832 Da were observed at the mass range from 3400 to 4400 Da (inset). Peaks higher than 4400 Da including the theoretically predicted peak of ~5058 Da corresponding to F-Nβ derived from S3 cleavage (asterisk, see B) were not observed. The major F-Nβ peak of 3832 Da was also identified by IP/MS analysis from conditioned media of K293 cells stably transfected with F-NEXT M1727V (data not shown). (B) Schematic representation of intramembranous cleavages of the mouse Notch-1 and human βAPP TMs. S4 cleavage of F-NEXT derivatives occurs predominantly between Ala1731 and Ala1732.

Table I. List of F-Nβ species found in conditioned media

M_r (observed)	F-Nβ	M_r (calculated)	Amino acid sequence
4334	F-Nβ_{1736}	4333.81	LRDYKDDDDKMVMKSEPVEPPLPSQ LHLMYVAAAAFVL^{1736}
4220	F-Nβ_{1735}	4220.66	LRDYKDDDDKMVMKSEPVEPPLPSQ LHLMYVAAAAFV^{1735}
4121	F-Nβ_{1734}	4121.53	LRDYKDDDDKMVMKSEPVEPPLPSQ LHLMYVAAAAF^{1734}
3974	F-Nβ_{1733}	3974.36	LRDYKDDDDKMVMKSEPVEPPLPSQ LHLMYVAAAA^{1733}
4045	F-Nβ_{1731}	4045.45	RGLRDYKDDDDKMVMKSEPVEPPLPSQ LHLMYVAA^{1731}
3832	**F-Nβ_{1731}**	**3832.22**	**LRDYKDDDDKMVMKSEPVEPPLPSQ LHLMYVAA^{1731}**
3563	F-Nβ_{1731}	3562.89	DYKDDDDKMVMKSEPVEPPLPSQ LHLMYVAA^{1731}
3760	F-Nβ_{1730}	3761.15	LRDYKDDDDKMVMKSEPVEPPLPSQ LHLMYVA^{1730}
3590	F-Nβ_{1728}	3590.95	LRDYKDDDDKMVMKSEPVEPPLPSQ LHLMY^{1728}
3427	F-Nβ_{1727}	3427.78	LRDYKDDDDKMVMKSEPVEPPLPSQ LHLM^{1727}

Bold letters indicate a peptide sequence and its properties of the major species.

S4 cleavage in a manner similar to the effects caused by FAD mutant PS on γ_{40}/γ_{42} cleavage. Interestingly, the two other FAD mutants analyzed produced individual changes in C-terminal heterogeneity of the S4 cleavage. While PS1 C92S elevated levels of a peptide terminating after amino acid 1734, PS1 L286V increased peptides terminating after amino acid 1735 and decreased the levels of F-Nβ1734 (Figure 4A). Therefore, the FAD mutants analyzed apparently cause individual and characteristic cleavage patterns. They all have in common the increased production of elongated species. Like Aβ42 production, the levels of elongated F-Nβ are most affected significantly by the very aggressive PS1 L166P mutation, which causes FAD in early adulthood (Moehlmann *et al.*, 2002). These effects are not restricted to K293 cells, since we also observed similar effects of FAD-associated PS2 mutations in Neuro2a cells (data not shown). To substantiate these findings further, we performed multiple independent experiments followed by a semi-quantitative analysis (see Materials and methods). This fully confirmed the primary observations. All FAD mutants analyzed affected the generation of the F-Nβ C-terminus in a highly reproducible and quantitative manner (Figure 4C).

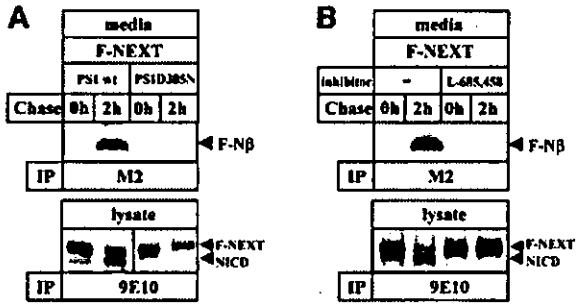

Fig. 3. F-Nβ is generated in a PS- and γ-secretase-dependent manner. (A) PS dependence of F-Nβ generation. K293 cells stably expressing wild-type PS1 or mutant PS1 D385N were stably transfected with the F-NEXT cDNA. Upper panel: F-Nβ generation was analyzed from conditioned media of metabolically labeled cells as described in Figure 1B. Lower panel: corresponding cell lysates were analyzed for NICD generation as described in Figure 1B. (B) γ-secretase dependence of F-Nβ generation. Upper panel: F-Nβ generation was analyzed as described in Figure 1B from conditioned media of K293 cells stably co-expressing F-NEXT and wild-type PS1 that were metabolically labeled in the presence or absence of γ-secretase inhibitor L-685,458 (1 μM). Lower panel: corresponding cell lysates were analyzed for NICD generation as described in Figure 1B.

Discussion

We have examined whether membrane-retained Notch fragments such as NEXT secrete peptides similar to Aβ upon NICD generation. Here we demonstrate that the NEXT derivative F-NEXT indeed undergoes an additional and unexpected cleavage at a novel site near the middle of the membrane, which results in the secretion of an Aβ-like peptide (Figure 5). Upon overexpression of F-NEXT, we identified several F-Nβ species with heterogeneous C-termini similar to Aβ. The major cleavage site was identified in the center of four sequential alanine residues between Ala1731 and Ala1732 in all cell lines analyzed so far (data herein and data not shown). Since it has been shown previously that NICD is generated by cleavage at S3 between Gly1743 and Val1744 (Schroeter *et al.*, 1998), one would have expected to detect a corresponding Nβ peptide terminating at Gly1743. However, in our study, we identified robust levels of peptides terminating at amino acid 1731, but failed to detect the secreted peptide corresponding to S3 cleavage in cultured media. Therefore, the intramembranous cleavage resulting in the immediate secretion of Nβ must be biochemically distinct from the previously identified S3 cleavage. Based on our findings, Nβ generation is therefore the result of a novel cleavage, and we consequently introduce the term S4 for this intramembranous cut.

Like AICD and Aβ production, generation of NICD and the novel Nβ are both dependent on PS-mediated γ-secretase processing. This is demonstrated by the significant reduction of Nβ generation upon the expression of a biologically inactive PS1 variant. Moreover, a highly potent γ-secretase inhibitor also blocked Nβ production. However, at present, we do not know the order of these cleavages. As discussed for AICD/Aβ generation (Sastre *et al.*, 2001), it is most likely that all the intramembranous γ-secretase cleavages occur simultaneously, since neither longer Aβ/Nβ nor AICD/NICD fragments have been identified so far.

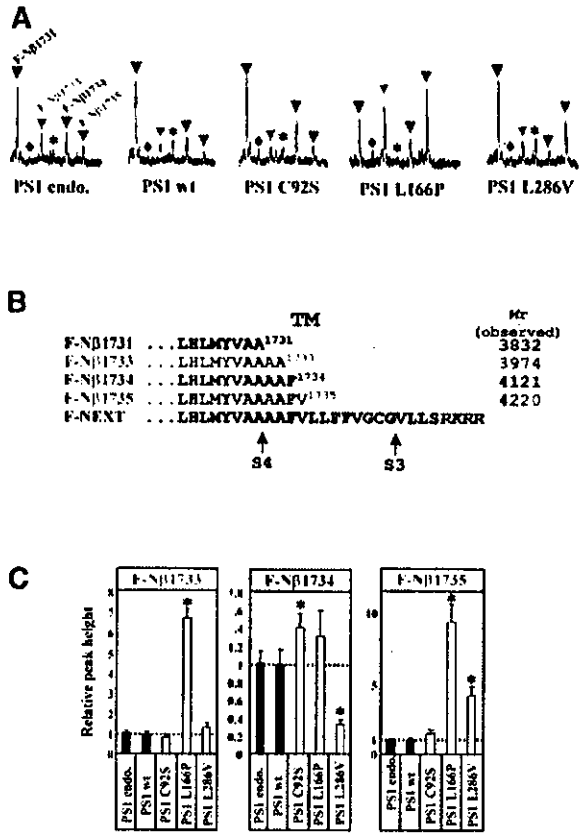

Fig. 4. PS1 FAD mutations affect the relative levels of elongated F-Nβ species. (A) MALDI-TOF MS spectra of F-Nβ species secreted from cells co-expressing F-NEXT and the indicated PS1 derivatives. Conditioned media were analyzed by IP/MS as described in Figure 2B. The mass range from ~3750 to ~4250 Da is shown. Black arrowhead, F-Nβ1731; colored arrowheads, F-Nβ1733 (green), F-Nβ1734 (blue) and F-Nβ1735 (red). The rhombus indicates the peak corresponding to F-Nβ1732 (molecular mass 3903 Da), and the asterisk indicates an F-Nβ1731 (molecular mass 4045 Da) species with a different N-terminus from that of the major F-Nβ1731 (molecular mass 3832 Da) species (compare Figure 2B and Table I). Note that FAD-associated PS1 mutations, in particular PS1 L166P, show an altered production of the various F-Nβ species. (B) C-termini of F-Nβ species affected by FAD-associated PS1 mutants. Sequences within the putative TM are shown. Black, F-Nβ1731; green, F-Nβ1733; blue, F-Nβ1734; red, F-Nβ1735. Arrows indicate S3 and S4. (C) Semi-quantitative analysis of elongated F-Nβ species. Conditioned media from cells expressing the indicated PS1 FAD-associated mutants (each medium amount for immunoprecipitation was normalized to contain the same level of F-Nβ1731; see Materials and methods) were analyzed by IP/MS. Peak heights corresponding to secreted F-Nβ1733, F-Nβ1734 and F-Nβ1735 were measured and are expressed relative to the peak height of the internal control (1 pmol bovine insulin β-chain; see Materials and methods). Asterisks indicate the significance of the increase and decrease of the various F-Nβ species relative to both endogenous/wild-type PS1-expressing cells ($P < 0.0001$; Students *t*-test). The data are the mean from five independent measurements.

Several PS-dependent γ-secretase substrates have been described. These include βAPP (De Strooper *et al.*, 1998), ErbB-4 (Ni *et al.*, 2001; Lee *et al.*, 2002), E-cadherin (Marambaud *et al.*, 2002), LRP (May *et al.*, 2002) and Notch-1–4 (De Strooper *et al.*, 1999; Mizutani *et al.*, 2001; Saxena *et al.*, 2001), and probably also CD44 (Okamoto *et al.*, 2001). Apparently, all these type I TM proteins release their C-terminal tails into the cytoplasm. Under

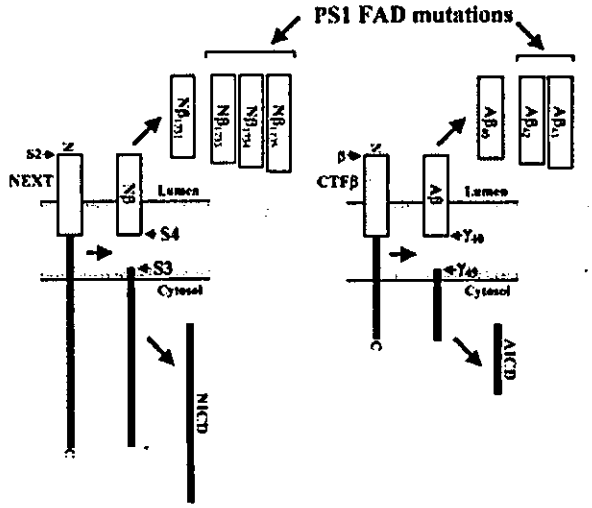

Fig. 5. Similar intramembranous cleavages of Notch-1 and βAPP. Following S2 cleavage, the Notch fragment NEXT is cleaved in a PS- and γ-secretase-dependent manner within the membrane at two major sites, S3 and S4. S3 cleavage occurs close to the cytosolic membrane border and leads to the liberation of NICD, whereas S4 cleavage occurs near the middle of the TM and causes the release of Nβ peptides. S3 and S4 cleavages are strikingly similar to γ_{49} and γ_{40} cleavages of CTFβ of βAPP, respectively. The generation of longer forms of Nβ and Aβ peptides ($A\beta_{42,43}$) are affected in a similar manner at least by some FAD-associated PS mutants.

in vivo conditions, some of the proteolytically liberated ICDs translocate to the nucleus (Schroeter *et al.*, 1998; Struhl and Adachi, 1998; Cao and Südhof, 2001; Ni *et al.*, 2001; Okamoto *et al.*, 2001; Lee *et al.*, 2002) where they do or may regulate transcription of target genes (reviewed in Steiner and Haass, 2001). The cleavage, which results in the liberation of ICDs, takes place very close to the cytoplasmic border of these proteins (Schroeter *et al.*, 1998; Gu *et al.*, 2001; Okamoto *et al.*, 2001; Sastre *et al.*, 2001; Yu *et al.*, 2001; Marambaud *et al.*, 2002; Weidemann *et al.*, 2002). In contrast, the γ-secretase cleavage of βAPP, which liberates Aβ, occurs in the middle of the TM. This apparent discrepancy has been used as an argument for the existence of two independent proteolytic enzymes involved in NICD generation and Aβ liberation (Yu *et al.*, 2001; reviewed in Sisodia and St George-Hyslop, 2002). Indeed, this idea may be supported by the selective inhibition of Aβ production without affecting Notch cleavage (Petit *et al.*, 2001). The consequence of these findings would be that Aβ generation and NICD (or even ICD production in general) is mediated by independent and distinct intramembrane cleaving proteases. However, our findings strongly support the idea that an evolutionarily conserved PS-dependent mechanism is involved in the two γ-secretase cleavages of Notch-1 and βAPP. Both result in the generation of the respective ICD (via cleavage close to the cytoplasmic border of the membrane) as well as the secretion of a small and hydrophobic peptide (via cleavage within the middle of the TM). The additional S4 intramembranous cleavage is also in agreement with recent findings demonstrating that an exchange of the βAPP TM with the Notch TM allows intramembranous γ-secretase processing at a position homologous to the site of Aβ40 generation (Zhang *et al.*, 2002). However, in the latter case, the cleavage was obtained several amino acids C-terminal of the S4 cleavage site determined in this study at a position corresponding to F-Nβ1735. The reason for this discrepancy is probably due to insertion of the Notch TM into an artificial βAPP backbone (Zhang *et al.*, 2002). In contrast, we used constitutively processed authentic Notch-1 derivatives mimicking NEXT. Finally, the selective inhibition of γ-secretase-mediated Aβ production (Petit *et al.*, 2001) has been challenged recently and it was clearly demonstrated that the inhibitors used do not directly affect PS-dependent γ-secretase cleavage and Aβ production (Esler *et al.*, 2002b).

Intramembranous endoproteolysis (S4/S3) of Notch-1 and βAPP shares many common features: (i) substrates of both S4/S3 and γ_{40}/γ_{49} cleavages are truncated extracellularly by shedding enzymes (reviewed in Mumm and Kopan, 2000; Steiner and Haass, 2000); (ii) S4/S3 (Figure 3) as well as γ_{40}/γ_{49} cleavages were found to be PS dependent; (iii) both the γ_{49} and S3 cleavages occur at analogous sites very close to the cytoplasmic border of the membrane (Schroeter *et al.*, 1998; Gu *et al.*, 2001; Sastre *et al.*, 2001; Yu *et al.*, 2001; Weidemann *et al.*, 2002); (iv) upon S4/S3 and γ_{40}/γ_{49} cleavages, the resulting fragments, Nβ/NICD (Figure 1) and Aβ/AICD, are released into the extracellular space or into the cytoplasm, respectively; (v) the extracellularly released fragments (Nβ/Aβ) do not correspond directly to the intracellularly released fragments (NICD/AICD), i.e. so far neither Nβ1743/Aβ49 nor NICD1732 (NICD starting from Ala1732, mouse Notch-1 numbering)/AICD59 (AICD starting from Ile41, Aβ numbering) have been identified; (vi) the C-termini of both peptides are heterogeneous; and, finally, (vii) FAD-associated mutants of PS1 cause the generation of C-terminally elongated Nβ fragments very similar to Aβ42 generated in the presence of FAD mutants (Figure 4). Due to these extensive similarities, it is very likely that the intramembraneous cleavages of both proteins occur by a common mechanism and are not mediated by different βAPP- and Notch-1-cleaving enzymes as proposed previously (Petit *et al.*, 2001, 2002a,b; Yu *et al.*, 2001; Taniguchi *et al.*, 2002; reviewed in Sisodia and St George-Hyslop, 2002). The conservation of this mechanism strongly suggests that at least Notch-1 and βAPP are cleaved twice by the same PS-dependent enzymatic mechanism. It certainly remains to be shown if the other γ-secretase substrates also undergo an additional intramembranous cleavage.

Finally, our data also support the hypothesis that PS harbors the catalytic site of γ-secretase and executes the cleavage of both βAPP and Notch-1. Interestingly, a very aggressive FAD-associated PS1 mutant (PS1 L166P), which causes an extreme increase of Aβ42 production, also dramatically shifts the corresponding cleavage of Notch-1. The most parsimonious explanation for this finding is a direct contact of PS with its substrates. Together with the finding that γ-secretase inhibitors bind to PS (Esler *et al.*, 2000; Li *et al.*, 2000), the observation of the 'critical aspartates' (Wolfe *et al.*, 1999), the similarity around the active site aspartate in TM7 of PSs to type 4 prepilin peptidases (Steiner *et al.*, 2000) and the finding

that mutations of Leu166 of PS1 affect the generation of AICD and NICD generation in a similar manner (Moehlmann *et al.*, 2002) suggest that PS is indeed the proteolytic subunit within the multicomponent γ-secretase complex. Such a complex requires additional factors for its assembly, stability and activity. One of these components is nicastrin (Yu et al., 2000), which is required for PS expression (Edbauer *et al.*, 2002; Hu *et al.*, 2002; Lopez-Schier and St Johnston, 2002), γ-secretase activity (Edbauer *et al.*, 2002) and Notch S3 cleavage (Chung and Struhl, 2001; Hu *et al.*, 2002; Lopez-Schier and St Johnston, 2002).

Materials and methods

Antibodies and reagents

The monoclonal antibodies 9E10 against the c-myc epitope and M2 against the FLAG epitope were obtained from Sigma (St Louis, MO). The γ-secretase inhibitor L-685,458, ([(2R,4R,5S)-2-benzyl-5-(Boc-amino)-4-hydroxy-6-phenyl-hexanoyl]-Leu-Phe-NH_2) was purchased from Bachem.

cDNA constructs

The cDNAs encoding the mouse Notch-1 variants NΔE and NICD carrying a C-terminal hexametric myc tag (Schroeter *et al.*, 1998) in pcDNA3-hygro (+) vector were described previously (Steiner *et al.*, 1999a). These Notch-1 variants contain the M1727V mutation (Kopan *et al.*, 1996). Mouse Notch-1 F-NEXT variants either containing or lacking the M1727V mutation were obtained by PCR-mediated mutagenesis. First, F-NEXT M1727V was generated using the ExSite PCR-based site-directed mutagenesis kit (Stratagene) using NΔE as the template and the primers 5′-P-ATCGTCGTCCTTGTAGTCTCTCAAG-CCTCTTGCGCCGAGCGCGGGCAGCAGCGTTAG-3′ and 5′-P-GAC-AAGATGGTGATGAAGAGTGAGCCGGTGGAGCCTCCGCTGCCC-TCGCAGCTG-3′. Subsequently, F-NEXT cDNA was generated by site-directed mutagenesis using the QuikChange site-directed mutagenesis kit (Stratagene) using F-NEXT M1727V cDNA as the template and the primers 5′-CCTCGCAGCTGCACCTCATGTACGTGGCAGCG-3′ and 5′-CGCGCCACGTACATGAGGTGCAGCTGCGAGG-3′. Each mutant was sequenced to verify successful mutagenesis.

Cell culture, cell lines and cDNA transfection

K293 cells stably expressing either wild-type PS1 (Okochi *et al.*, 2000), PS1 C92S (Okochi *et al.*, 2000), PS1 L166P (Moehlmann *et al.*, 2002), PS1 L286V (Kulic *et al.*, 2000) or PS1 D385N (Steiner *et al.*, 1999b) were generated and cultured as described. Stable transfections with NΔE, NICD and F-NEXT cDNA constructs were carried out using Lipofectamine 2000 (Invitrogen) according to the supplier's instructions.

Analysis of Notch-1 metabolites

Confluent cells in a 10 cm dish were analyzed for Notch-1 metabolites in pulse–chase experiments. Following starvation in methionine- and serum-free minimal essential medium (MEM) for 40 min, cells subsequently were metabolically labeled with 400 μCi of [^{35}S]methionine/cysteine (Redivue Promix, Amersham) for 1 h in methionine- and serum-free MEM and chased for 2 h in Dulbecco's modified Eagle's medium (DMEM) containing 10% fetal calf serum (FCS) and excess amounts of unlabeled methionine. Conditioned media were collected, immediately put on ice and, after a clarifying spin at 3000 *g* and addition of a protease inhibitor cocktail (1:1000; Sigma) and 0.025% of sodium azide, subjected to immunoprecipitation with anti-FLAG M2 agarose (Sigma). Immunoprecipitates were separated on 10–20% Tris-tricine gels (Invitrogen) and analyzed for F-Nβ species by fluorography. Cell lysates were prepared as described (Okochi *et al.*, 2000) and analyzed for NΔE, F-NEXT and derivatives thereof, and NICD by immunoprecipitation with antibody 9E10 as described (Steiner *et al.*, 1999a). γ-Secretase dependence of Notch-1 endoproteolysis was analyzed using γ-secretase inhibitor L-685,458 (1 μM; Shearman *et al.*, 2000), which was added to the culture media 2 h before starvation and present throughout the starvation, pulse and chase periods.

Combined immunoprecipitation/MALDI-TOF MS (IP/MS) analysis of Nβ species

Cell lines stably expressing F-NEXT derivatives were grown in 20 cm dishes. After reaching confluence, the culture media were replaced with 24 ml of 10% FCS/DMEM and media were incubated for 3 h. A 20 ml aliquot of the conditioned media was collected, immediately put on ice and subjected to a clarifying spin. Following addition of a protease inhibitor mix (1:1000, Sigma) and 0.025% sodium azide, conditioned media were immunoprecipitated with M2 agarose for 4 h at 4°C. Immunoprecipitates were washed three times for 10 min at 4°C with wash buffer 1 (0.1% *N*-octylglucoside, 140 mM NaCl, 10 mM Tris pH 8.0, 0.025% sodium azide) and once with wash buffer 2 (10 mM Tris pH 8.0, 0.025% sodium azide). Immunoprecipitated peptides were eluted with trifluoroacetic acid/acetonitrile/water (1:20:20) saturated with α-cyano-4-hydroxy cinnamic acid. The dissolved samples were dried on a stainless plate and subjected to MALDI-TOF MS analysis. The MS peak heights and molecular masses were calibrated with angiotensin (Sigma) and bovine insulin β-chain (Sigma).

Semi-quantitative analysis of F-Nβ species

Conditioned media from the respective K293 cells co-expressing F-NEXT/PS were collected and aliquots of the conditioned media were subjected to IP/MS analysis. The peak heights of F-Nβ1731 in the MS spectra were measured and its peak heights relative to the peak height of 1 pmol bovine insulin β-chain (internal control) were calculated. These relative peak heights were used to calculate the relative levels of the F-Nβ1731 species contained in each conditioned medium of the respective F-NEXT/PS-transfected cells. Subsequently, the amounts of the conditioned media were adjusted to contain the same levels of F-Nβ1731 using a standard curve for F-Nβ1731, and again subjected to IP/MS analysis. After confirming that the F-Nβ1731 peak has the same height as the peak of the internal control, peak heights corresponding to C-terminally longer F-Nβ species (F-Nβ1733, F-Nβ1734 or F-Nβ1735) were measured and its peak heights relative to the internal control were calculated. Relative peak heights of F-Nβ species obtained from endogenous/wild-type PS1 and PS1 FAD-associated mutants were compared.

Acknowledgements

We wish to thank Drs Junji Takeda, Hiroshi Mori and Shinji Tagami for critically reading the manuscript, Yumi Satoh, Nuripa Aidaralieva and Gabi Basset for technical assistance, and Dr Raphael Kopan for the NΔE and NICD constructs. This work was supported by grants from the Ministry of Health and Welfare (14121601 to M.T. and M.O., and 13080101 to M.T.), the Ministry of Education, Science, Culture and Sports (14017060 and 14770499 to M.O.), the Deutsche Forschungsgemeinschaft (Priority program on 'Cellular Mechanisms of Alzheimer's Disease' to C.H. and H.S.) and the American Health Association Foundation (AHAF to C.H. and H.S).

References

Beher,D., Wrigley,J.D., Nadin,A., Evin,G., Masters,C.L., Harrison,T., Castro,J.L. and Shearman,M.S. (2001) Pharmacological knock-down of the presenilin 1 heterodimer by a novel γ-secretase inhibitor: implications for presenilin biology. *J. Biol. Chem.*, **276**, 45394–45402.

Brou,C. *et al.* (2000) A novel proteolytic cleavage involved in Notch signaling: the role of the disintegrin-metalloprotease TACE. *Mol. Cell*, **5**, 207–216.

Cao,X. and Sudhof,T.C. (2001) A transcriptionally active complex of APP with Fe65 and histone acetyltransferase Tip60. *Science*, **293**, 115–120.

Capell,A., Steiner,H., Romig,H., Keck,S., Baader,M., Grim,M.G., Baumeister,R. and Haass,C. (2000) Presenilin-1 differentially facilitates endoproteolysis of the β-amyloid precursor protein and Notch. *Nat. Cell Biol.*, **2**, 205–211.

Chung,H.M. and Struhl,G. (2001) Nicastrin is required for presenilin-mediated transmembrane cleavage in *Drosophila*. *Nat. Cell Biol.*, **3**, 1129–1132.

Cupers,P., Orlans,I., Craessaerts,K., Annaert,W. and De Strooper,B. (2001) The amyloid precursor protein (APP)-cytoplasmic fragment generated by γ-secretase is rapidly degraded but distributes partially in a nuclear fraction of neurones in culture. *J. Neurochem.*, **78**, 1168–1178.

De Strooper,B., Saftig,P., Craessaerts,K., Vanderstichele,H., Guhde,G., Annaert,W., Von Figura,K. and Van Leuven,F. (1998) Deficiency of presenilin-1 inhibits the normal cleavage of amyloid precursor protein. *Nature*, **391**, 387–390.

De Strooper,B. *et al.* (1999) A presenilin-1-dependent γ-secretase-like protease mediates release of Notch intracellular domain. *Nature*, **398**, 518–522.

Edbauer,D., Winkler,E., Haass,C. and Steiner,H. (2002) Presenilin and nicastrin regulate each other and determine amyloid β-peptide production via complex formation. *Proc. Natl Acad. Sci. USA*, **99**, 8666–8671.

Esler,W.P. and Wolfe,M.S. (2001) A portrait of Alzheimer secretases—new features and familiar faces. *Science*, **293**, 1449–1454.

Esler,W.P. *et al.* (2000) Transition-state analogue inhibitors of γ-secretase bind directly to presenilin-1. *Nat. Cell Biol.*, **2**, 428–434.

Esler,W.P. *et al.* (2002a) Amyloid-lowering isocoumarins are not direct inhibitors of γ-secretase. *Nat. Cell Biol.*, **4**, 110–111.

Esler,W.P., Kimberly,W.T., Ostaszewski,B.L., Ye,W., Diehl,T.S., Selkoe,D.J. and Wolfe,M.S. (2002b) Activity-dependent isolation of the presenilin–γ-secretase complex reveals nicastrin and a γ-substrate. *Proc. Natl Acad. Sci. USA*, **99**, 2720–2725.

Gao,Y. and Pimplikar,S.W. (2001) The γ-secretase-cleaved C-terminal fragment of amyloid precursor protein mediates signaling to the nucleus. *Proc. Natl Acad. Sci. USA*, **98**, 14979–14984.

Gu,Y., Misonou,H., Sato,T., Dohmae,N., Takio,K. and Ihara,Y. (2001) Distinct intramembrane cleavage of the β-amyloid precursor protein family resembling γ-secretase-like cleavage of Notch. *J. Biol. Chem.*, **276**, 35235–35238.

Haass,C. and Selkoe,D.J. (1993) Cellular processing of β-amyloid precursor protein and the genesis of amyloid β-peptide. *Cell*, **75**, 1039–1042.

Haass,C., Hung,A.Y., Schlossmacher,M.G., Teplow,D.B. and Selkoe, D.J. (1993) β-amyloid peptide and a 3-kDa fragment are derived by distinct cellular mechanisms. *J. Biol. Chem.*, **268**, 3021–3024.

Hu,Y., Ye,Y. and Fortini,M.E. (2002) Nicastrin is required for γ-secretase cleavage of the *Drosophila* Notch receptor. *Dev. Cell*, **2**, 69–78.

Kimberly,W.T., Zheng,J.B., Guenette,S.Y. and Selkoe,D.J. (2001) The intracellular domain of the β-amyloid precursor protein is stabilized by Fe65 and translocates to the nucleus in a Notch-like manner. *J. Biol. Chem.*, **276**, 40288–40292.

Kopan,R., Schroeter,E.H, Weintraub,H. and Nye,J.S. (1996) Signal transduction by activated mNotch: importance of proteolytic processing and its regulation by the extracellular domain. *Proc. Natl Acad. Sci. USA*, **93**, 1683–1688.

Kulic,L., Walter,J., Multhaup,G., Teplow,D.B., Baumeister,R., Romig,H., Capell,A., Steiner,H. and Haass,C. (2000) Separation of presenilin function in amyloid β-peptide generation and endoproteolysis of Notch. *Proc. Natl Acad. Sci. USA*, **97**, 5913–5918.

Lee,H.J., Jung,K.M., Huang,Y.Z., Bennett,L.B., Lee,J.S., Mei,L. and Kim,T.W. (2002) Presenilin-dependent γ-secretase-like intramembrane cleavage of ErbB4. *J. Biol. Chem.*, **277**, 6318–6323.

Li,Y.M. *et al.* (2000) Presenilin 1 is linked with γ-secretase activity in the detergent solubilized state. *Proc. Natl Acad. Sci. USA*, **97**, 6138–6143.

Lopez-Schier,H. and St Johnston,D. (2002) *Drosophila* nicastrin is essential for the intramembranous cleavage of Notch. *Dev. Cell*, **2**, 79–89.

Marambaud,P. *et al.* (2002) A presenilin-1/γ-secretase cleavage releases the E-cadherin intracellular domain and regulates disassembly of adherens junctions. *EMBO J.*, **21**, 1948–1956.

Martys-Zage,J.L., Kim,S.H., Berechid,B., Bingham,S.J., Chu,S., Sklar,J., Nye,J. and Sisodia,S.S. (2000) Requirement for presenilin 1 in facilitating Jagged 2-mediated endoproteolysis and signaling of Notch 1. *J. Mol. Neurosci.*, **15**, 189–204.

May,P., Reddy,Y.K. and Herz,J. (2002) Proteolytic processing of LRP mediates regulated release of its intracellular domain. *J. Biol. Chem.*, **277**, 18736–18743.

Mizutani,T., Taniguchi,Y., Aoki,T., Hashimoto,N. and Honjo,T. (2001) Conservation of the biochemical mechanisms of signal transduction among mammalian Notch family members. *Proc. Natl Acad. Sci. USA*, **98**, 9026–9031.

Moehlmann,T. *et al.* (2002) Presenilin-1 mutations of leucine 166 equally affect the generation of Notch and APP intracellular domains independent of their effect on Aβ42 production. *Proc. Natl Acad. Sci. USA*, **99**, 8025–8030.

Mumm,J.S. and Kopan,R. (2000) Notch signaling: from the outside in. *Dev. Biol.*, **228**, 151–165.

Mumm,J.S., Schroeter,E.H., Saxena,M.T., Griesemer,A., Tian,X., Pan,D.J., Ray,W.J. and Kopan,R.A. (2000) A ligand-induced extracellular cleavage regulates γ-secretase-like proteolytic activation of Notch1. *Mol. Cell*, **5**, 197–206.

Ni,C.Y., Murphy,M.P., Golde,T.E. and Carpenter,G. (2001) γ-secretase cleavage and nuclear localization of ErbB-4 receptor tyrosine kinase. *Science*, **294**, 2179–2181.

Okamoto,I., Kawano,Y., Murakami,D., Sasayama,T., Araki,N., Miki,T., Wong,A,J. and Saya,H. (2001) Proteolytic release of CD44 intracellular domain and its role in the CD44 signaling pathway. *J. Cell Biol.*, **155**, 755–762.

Okochi,M., Eimer,S., Bottcher,A., Baumeister,R., Romig,H., Walter,J., Capell,A., Steiner,H. and Haass,C. (2000) A loss of function mutant of the presenilin homologue SEL-12 undergoes aberrant endoproteolysis in *Caenorhabditis elegans* and increases Aβ 42 generation in human cells. *J. Biol. Chem.*, **275**, 40925–40932.

Petit,A., Bihel,F., Alves da Costa,C., Pourquie,O., Checler,F. and Kraus,J.L. (2001) New protease inhibitors prevent γ-secretase-mediated production of Aβ40/42 without affecting Notch cleavage. *Nat. Cell Biol.*, **3**, 507–511.

Petit,A., Dumanchin-Njock,C., Andrau,D., Da Costa,C.A. and Checler,F. (2002a) Amyloid-lowering isocoumarins are not direct inhibitors of γ-secretase. *Nat. Cell Biol.*, **4**, 111–112.

Petit,A., St George-Hyslop,P., Fraser,P. and Checler,F. (2002b) γ-secretase-like cleavages of Notch and βAPP are mutually exclusive in human cells. *Biochem. Biophys. Res. Commun.*, **290**, 1408–1410.

Sastre,M., Steiner,H., Fuchs,K., Capell,A., Multhaup,G., Condron,M.M., Teplow,D.B. and Haass,C. (2001) Presenilin-dependent γ-secretase processing of β-amyloid precursor protein at a site corresponding to the S3 cleavage of Notch. *EMBO rep.* **2**, 835–841.

Saxena,M.T., Schroeter,E.H., Mumm,J.S. and Kopan,R. (2001) Murine notch homologs (N1–4) undergo presenilin-dependent proteolysis. *J. Biol. Chem.*, **276**, 40268–40273.

Schroeter,E.H., Kisslinger,J.A. and Kopan,R. (1998) Notch-1 signalling requires ligand-induced proteolytic release of intracellular domain. *Nature*, **393**, 382–386.

Selkoe,D.J. (2001) Alzheimer's disease: genes, proteins and therapy. *Physiol. Rev.*, **81**, 741–766.

Shearman,M.S. *et al.* (2000) L-685,458, an aspartyl protease transition state mimic, is a potent inhibitor of amyloid β-protein precursor γ-secretase activity. *Biochemistry*, **39**, 8698–8704.

Sisodia,S.S. and St George-Hyslop,P.H. (2002) γ-secretase, Notch, Aβ and Alzheimer's disease: where do the presenilins fit in? *Nat. Rev. Neurosci.*, **3**, 281–290.

Song,W., Nadeau,P., Yuan,M., Yang,X., Shen,J. and Yankner,B.A. (1999) Proteolytic release and nuclear translocation of Notch-1 are induced by presenilin-1 and impaired by pathogenic presenilin-1 mutations. *Proc. Natl Acad. Sci. USA*, **96**, 6959–6963.

Steiner,H. and Haass,C. (2000) Intramembrane proteolysis by presenilins. *Nat. Rev. Mol. Cell. Biol.*, **1**, 217–224.

Steiner,H. and Haass,C. (2001) Nuclear signaling: a common function of presenilin substrates? *J. Mol. Neurosci.*, **17**, 193–198.

Steiner,H. *et al.* (1999a) A loss of function mutation of presenilin-2 interferes with amyloid β-peptide production and Notch signaling. *J. Biol. Chem.*, **274**, 28669–28673.

Steiner,H., Romig,H., Pesold,B., Baader,M., Citron,M., Loetscher,H., Jacobsen,H. and Haass,C. (1999b) Amyloidogenic function of Alzheimer's disease associated presenilin-1 in the absence of endoproteolysis. *Biochemistry*, **38**, 14600–14605.

Steiner,H. *et al.* (2000) Glycine 384 is required for presenilin-1 function and is conserved in bacterial polytopic aspartyl proteases. *Nat. Cell Biol.*, **2**, 848–851.

Struhl,G. and Adachi,A. (1998) Nuclear access and action of Notch *in vivo*. *Cell*, **93**, 649–660.

Taniguchi,Y. *et al.* (2002) Notch receptor cleavage depends on but is not directly executed by presenilins. *Proc. Natl Acad. Sci. USA*, **99**, 4014–4019.

Wang,R., Sweeney,D., Gandy,S.E. and Sisodia,S.S. (1996) The profile of soluble amyloid β protein in cultured cell media. Detection and quantification of amyloid β protein and variants by immunoprecipitation–mass spectrometry. *J. Biol. Chem.*, **271**, 31894–31902.

Weidemann,A., Eggert,S., Reinhard,F.B., Vogel,M., Paliga,K., Baier,G., Masters,C.L., Beyreuther,K. and Evin,G.A. (2002) Novel ε-cleavage

within the transmembrane domain of the Alzheimer amyloid precursor protein demonstrates homology with Notch processing. *Biochemistry*, **41**, 2825–2835.

Wolfe,M.S., Xia,W., Ostaszewski,B.L., Diehl,T.S., Kimberly,W.T. and Selkoe,D.J. (1999) Two transmembrane aspartates in presenilin-1 required for presenilin endoproteolysis and γ-secretase activity. *Nature*, **398**, 513–517.

Yu,C., Kim,S.H., Ikeuchi,T., Xu,H., Gasparini,L., Wang,R. and Sisodia,S.S. (2001) Characterization of a presenilin-mediated amyloid precursor protein carboxyl-terminal fragment γ. Evidence for distinct mechanisms involved in γ-secretase processing of the APP and Notch1 transmembrane domains. *J. Biol. Chem.*, **276**, 43756–43760.

Yu,G. *et al.* (2000) Nicastrin modulates presenilin-mediated notch/glp-1 signal transduction and βAPP processing. *Nature*, **407**, 48–54.

Zhang,J., Ye,W., Wang,R., Wolfe,M.S., Greenberg,B.D. and Selkoe,D.J. (2002) Proteolysis of chimeric β-amyloid precursor proteins containing the Notch transmembrane domain yields amyloid β-like peptides. *J. Biol. Chem.*, **277**, 15069–15075.

Received July 2, 2002; revised August 14, 2002; accepted August 21, 2002

The EMBO Journal Vol. 21 No. 20 pp. 5408–5416, 2002

Presenilins mediate a dual intramembranous γ-secretase cleavage of Notch-1

Masayasu Okochi, Harald Steiner[1], Akio Fukumori, Hisashi Tanii, Taisuke Tomita[2], Toshihisa Tanaka, Takeshi Iwatsubo[2], Takashi Kudo, Masatoshi Takeda[3] and Christian Haass[1]

Department of Post-Genomics and Diseases, Division of Psychiatry and Behavioral Proteomics, Osaka University Graduate School of Medicine, 565-0871 Osaka, [2]Department of Neuropathology and Neuroscience, Graduate School of Pharmaceutical Sciences, University of Tokyo, 113-0033 Tokyo, Japan and [1]Adolf-Butenandt-Institute, Department of Biochemistry, Laboratory for Alzheimer's and Parkinson's Disease Research, Ludwig-Maximilians-University, D-80336 Munich, Germany

[3]Corresponding author
e-mail: mtakeda@psy.med.osaka-u.ac.jp

Following ectodomain shedding, Notch-1 undergoes presenilin (PS)-dependent constitutive intramembranous endoproteolysis at site-3. This cleavage is similar to the PS-dependent γ-secretase cleavage of the β-amyloid precursor protein (βAPP). However, topological differences in cleavage resulting in amyloid β-peptide (Aβ) or the Notch-1 intracellular domain (NICD) indicated independent mechanisms of proteolytic cleavage. We now demonstrate the secretion of an N-terminal Notch-1 Aβ-like fragment (Nβ). Analysis of Nβ by MALDI-TOF MS revealed that Nβ is cleaved at a novel site (site-4, S4) near the middle of the transmembrane domain. Like the corresponding cleavage of βAPP at position 40 and 42 of the Aβ domain, S4 cleavage is PS dependent. The precision of this cleavage is affected by familial Alzheimer's disease-associated PS1 mutations similar to the pathological endoproteolysis of βAPP. Considering these similarities between intramembranous processing of Notch and βAPP, we conclude that these proteins are cleaved by a common mechanism utilizing the same protease, i.e. PS/γ-secretase.

Keywords: Notch signaling/Notch-1-β peptide/presenilin/γ-secretase/site-4 cleavage

Introduction

The Notch cell surface receptors are type I transmembrane domain (TM) proteins that are critically required for a variety of signaling events during embryogenesis and in adulthood (reviewed in Mumm and Kopan, 2000). Notch receptors undergo a cascade of endoproteolytic cleavages required for Notch signaling (reviewed in Mumm and Kopan, 2000). Upon binding of membrane-anchored ligands from the DSL (Delta/Serrate/Lag-2) family, Notch receptors undergo consecutive cleavages at site-2 (S2) and site-3 (S3) (reviewed in Mumm and Kopan, 2000). Cleavage of mouse Notch-1 at S2 occurs in its ectodomain by TACE [tumor necrosis factor-α (TNF-α)-converting enzyme], a member of the ADAM (a disintegrin and metalloprotease domain) family ~12 amino acids distant from the TM. This 'ectodomain shedding' event results in the generation of NEXT (Notch extracellular truncation; Brou *et al.*, 2000; Mumm *et al.*, 2000), that is cleaved subsequently at S3 within the TM close to the cytoplasmic border (Schroeter *et al.*, 1998). Cleavage of Notch at S3 liberates NICD (Notch intracellular domain), that translocates to the nucleus, where it is involved in target gene transcription (reviewed in Mumm and Kopan, 2000). S3 cleavage strictly depends on the biological activity of the presenilin (PS) proteins (reviewed in Steiner and Haass, 2000), which may contribute the catalytic site of γ-secretase, an unusual intramembrane-cleaving aspartyl protease complex (Wolfe *et al.*, 1999; Li *et al.*, 2000; Steiner *et al.*, 2000; Esler *et al.*, 2002a).

Beside the Notch-1–4 receptors (De Strooper *et al.*, 1999; Mizutani *et al.*, 2001; Saxena *et al.*, 2001), several other type I TM proteins have been identified as substrates for PS-dependent endoproteolysis, including the Alzheimer's disease (AD)-associated β-amyloid protein precursor (βAPP) (De Strooper *et al.*, 1998), ErbB-4 (Ni *et al.*, 2001; Lee *et al.*, 2002), E-cadherin (Marambaud *et al.*, 2002) and LRP (May *et al.*, 2002). These proteins undergo 'ectodomain shedding' in their large extracellular domains, prior to the consecutive PS-dependent cleavage within the TM. In the case of βAPP, these cleavages are mediated by α-secretase and β-secretase (reviewed in Esler and Wolfe, 2001). Cleavage of βAPP by α- and β-secretase (BACE) results in the generation of the respective βAPP C-terminal fragments (CTFs), CTFα and CTFβ, which are the direct substrates for γ-secretase cleavage. Cleavage of CTFβ and CTFα by γ-secretase occurs in the middle of the TM and leads to the liberation of Aβ and p3 peptides (Haass and Selkoe, 1993), respectively. Aβ is deposited in the brain of AD patients in 'senile plaques', an invariant pathological hallmark of AD (reviewed in Selkoe, 2001). Recently, the elusive C-terminal cleavage product of γ-secretase, AICD (βAPP intracellular domain), has been identified and characterized. Surprisingly, AICD results from PS-dependent γ-secretase cleavage of βAPP–CTFs predominantly after Leu49 (Aβ numbering). This cleavage is almost identical to the S3 cleavage of Notch-1 (Gu *et al.*, 2001; Sastre *et al.*, 2001; Yu *et al.*, 2001; Weidemann *et al.*, 2002) and does not occur after Val40 and Ala42 (Aβ numbering) as predicted. Thus, γ-secretase cleaves the βAPP TM at several sites: one in the middle after position 40 (γ_{40}) and 42 (γ_{42}) (with major γ_{40} and minor γ_{42} cleavage) and one close to the cytoplasmic border after position 49 (γ_{49}) of the Aβ domain. Interestingly, AICD may translocate to the nucleus where it could have a role in transcriptional

regulation (Cao and Südhof, 2001; Cupers *et al.*, 2001; Kimberly *et al.*, 2001; Gao and Pimplikar, 2002) similar to NICD.

Because of these striking similarities between Notch and βAPP endoproteolysis, we hypothesized that an Aβ/p3-like species (called Notch β-peptide, Nβ) derived from NEXT intramembranous proteolysis may be secreted into the extracellular space. Here we report the identification and characterization of secreted Nβ peptides derived from endoproteolysis of NEXT derivatives. Sequence analysis revealed that Nβ is derived from endoproteolytic cleavage near the middle of the Notch-1 TM at site-4 (S4), which is 12 amino acid residues upstream of S3. Like S3 cleavage, S4 cleavage occurs in a PS- and γ-secretase-dependent manner. Strikingly, familial AD (FAD)-associated PS mutants known to cause the increased production of C-terminally elongated pathogenic $A\beta_{42}$ also affect the generation of C-terminally elongated Nβ variants, supporting a direct role for PS in the proteolytic cleavage of Notch-1 and βAPP.

Results

Detection of a secreted Notch-1 Aβ-like peptide

Given the similarities between the endoproteolytic processing of βAPP and Notch, we hypothesized that Aβ-like peptides derived from an S2-cleaved membrane-retained NEXT fragment might be secreted into the extracellular space. In order to investigate this, we stably transfected human embryonic kidney 293 (K293) cells with F-NEXT, an N-terminally FLAG-tagged NΔE variant (Figure 1A). We first investigated whether F-NEXT undergoes constitutive S3 endoproteolysis like the well-characterized NΔE variant (Kopan *et al.*, 1996). F-NEXT- and NΔE-expressing cells were pulse labeled with [^{35}S]methionine for 1 h and chased for 2 h. Immunoprecipitation with anti-myc antibody 9E10 revealed robust amounts of F-NEXT and NΔE (Figure 1B). NICD was produced during the pulse labeling and the chase period and accumulated after 2 h of chase (Figure 1B), consistent with previous results (Steiner *et al.*, 1999a). To analyze secretion of Notch-1 peptides, the corresponding conditioned media were immunoprecipitated with the anti-FLAG antibody M2. Strikingly, robust amounts of a peptide of a molecular mass of ~4 kDa were observed in the conditioned media of F-NEXT-expressing cells after a 2 h chase period (Figure 1B). This peptide is secreted in a time-dependent manner (Figure 1C) similar to Aβ (Haass *et al.*, 1993) and did not accumulate inside the cells (Figure 1C). As expected, no M2-precipitable peptides were detected in the corresponding media of NΔE-expressing cells, demonstrating the specificity of the isolation procedure (Figure 1B). Untagged NΔE was also processed into a secreted peptide (data not shown). We conclude from these data that NEXT undergoes constitutive endoproteolysis resulting in the secretion of a peptide, which we term Notch-1-β peptide (Nβ) in analogy to Aβ.

Nβ is derived from intramembranous proteolysis at a novel cleavage site

We hypothesized that Notch-1 may undergo a γ_{40} analogous cleavage further N-terminal of S3, which could result in Nβ secretion. To determine the exact cleavage site of F-NEXT, we performed matrix-associated laser desorption ionization-time of flight mass spectrometry (MALDI-TOF MS) analysis of the secreted FLAG-tagged Nβ (F-Nβ). MALDI-TOF MS analysis of M2-immunoprecipitated F-Nβ revealed a major peak of a molecular mass of 3832 Da among several minor peaks, indicating heterogeneous processing of the Notch-1 TM (Figure 2A, inset; see Table I for the F-Nβ peptides identified in this study). Interestingly, the heterogeneity of the F-Nβ C-termini (see Table I) is similar to the C-terminal heterogeneity observed in secreted Aβ species (Wang *et al.*, 1996). Strikingly, the major F-Nβ peak corresponded to a peptide ending with Ala1731 (mouse Notch-1 numbering, Figure 2), indicating that F-Nβ is derived by a predominant cleavage at a novel site between Ala1731 and Ala1732, and not by cleavage at S3 between Gly1743 and Val1744 as predicted. This is consistent with the lack of any detectable F-Nβ species with a C-terminus corresponding to Gly1743 (see asterisk in Figure 2A). Identical results were obtained when Neuro2a, COS or CHO cells were used in this analysis (data not shown). Thus, these data strongly suggest that Notch-1, like βAPP, undergoes several distinct intramembranous cleavages: one close to the cytoplasmic border (S3) of the TM and a novel heterogeneous cut near the middle of the TM, which we now term site-4 (S4) cleavage (Figure 2B).

S4 cleavage is PS/γ-secretase dependent

Since $\gamma_{40/42}$ cleavage of βAPP has been shown to require PS activity (reviewed in Steiner and Haass, 2000), we next investigated whether S4 cleavage is also PS dependent. K293 cells expressing biologically inactive PS1 D385N (Steiner *et al.*, 1999b), which lacks one of the two putative active site aspartates (Wolfe *et al.*, 1999), were stably transfected with F-NEXT and analyzed for the generation of F-Nβ. Strikingly, F-Nβ generation was almost completely inhibited in cells expressing PS1 D385N (Figure 3A, upper panel). Consistent with previous results (Capell *et al.*, 2000), NICD production was also significantly reduced (Figure 3A, lower panel). To confirm further the PS/γ-secretase dependence of F-Nβ generation, we treated cells with the γ-secretase inhibitor L-685,458 (Shearman *et al.*, 2000). When L-685,458 was added to the pulse–chase experiment, an almost complete inhibition of F-Nβ generation was observed (Figure 3B, upper panel). As expected, NICD generation (Martys-Zage *et al.*, 2000; Beher *et al.*, 2001) was also blocked (Figure 3B, lower panel). Taken together, these results demonstrate that F-Nβ generation occurs by cleavage at S4 in a PS/γ-secretase-dependent manner similar to the generation of Aβ.

FAD-associated PS mutations affect S4 cleavage

All FAD-associated PS mutations analyzed so far result in the increased secretion of Aβ42 (reviewed in Steiner and Haass, 2000). We therefore investigated whether the PS-dependent S4 cleavage is also influenced by FAD-associated PS mutants. F-NEXT was stably transfected into K293 cells expressing wild-type PS1 or the FAD-associated PS1 mutants PS1 C92S, PS1 L166P and PS1 L286V (Kulic *et al.*, 2000; Okochi *et al.*, 2000; Moehlmann *et al.*, 2002). In particular, the L166P mutation was chosen because it not only causes one of

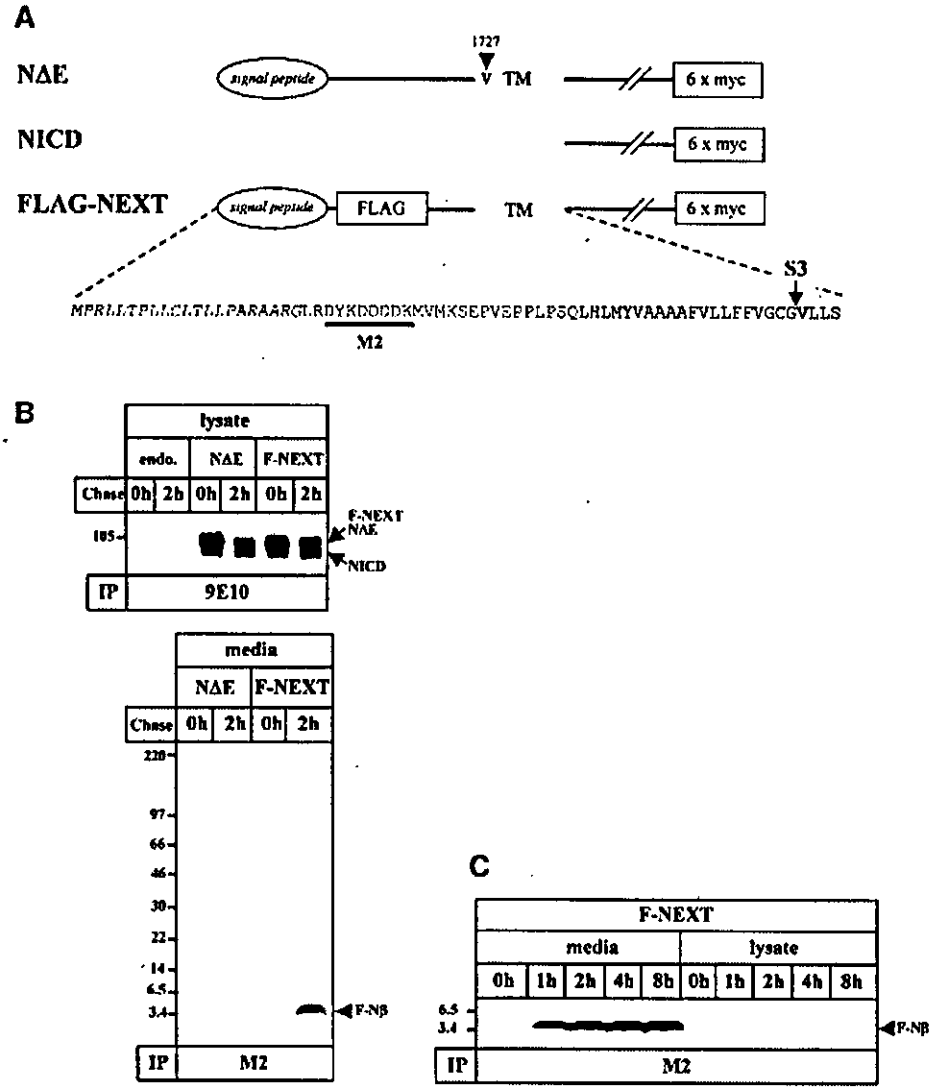

Fig. 1. Detection of a secreted Notch-1 fragment. (A) Schematic representation of NΔE, NICD and F-NEXT. All three mouse Notch-1 variants contain a hexametric myc tag at the C-terminus to facilitate detection. F-NEXT is a NΔE variant that contains an insertion of the FLAG epitope and two adjacent methionine residues after the signal peptide sequence to facilitate the detection of secreted Notch-1 fragments. An arrowhead indicates the M1727V mutation present in NΔE (Kopan *et al.*, 1996). An arrow shows S3, and the critical valine is shown in bold. The recognition site of the anti-FLAG antibody M2 is represented by the black bar. (B) Detection of a secreted FLAG-tagged Notch-1 fragment (F-Nβ) derived from F-NEXT. Untransfected K293 cells or K293 cells stably expressing NΔE or F-NEXT were pulse labeled with [^{35}S]methionine for 1 h and chased for 0 and 2 h. Upper panel: cell lysates were immunoprecipitated with anti-myc antibody 9E10. F-NEXT and NΔE undergo S3 cleavage with similar efficiency. Note that in this pulse–chase paradigm, NICD generation is detectable after pulse labeling for 1 h without chase. Lower panel: conditioned media from K293 cells stably expressing NΔE or F-NEXT were immunoprecipitated with anti-FLAG M2 agarose. (C) Time-dependent secretion of F-Nβ. K293 cells stably expressing F-NEXT were pulse labeled with [^{35}S]methionine for 1 h and chased for the indicated times. F-Nβ was analyzed in conditioned media, and cell lysates by immunoprecipitation with anti-FLAG M2 agarose. A longer exposure revealed that very low amounts of F-Nβ were also detectable in the cell lysates (data not shown). Identical results were obtained with F-NEXT M1727V (data not shown).

the strongest increases in Aβ42 generation, but also significantly inhibits S3 cleavage (Moehlmann *et al.*, 2002). Thus, this mutation allows investigation of whether a PS mutant that inhibits S3 cleavage also affects S4 cleavage. We analyzed the conditioned media of cells co-expressing the PS1 derivatives and F-NEXT by MALDI-TOF MS for putative alterations in the C-termini of F-Nβ. Strikingly, this revealed significant changes in the C-terminal cleavage pattern of Nβ produced in cells expressing wild-type or FAD mutant PS1 (Figure 4A). Specifically, the PS1 L166P mutation, which causes an extremely strong increase of Aβ42 generation (Moehlmann *et al.*, 2002), also produced strongly increased levels of elongated F-Nβ peptides. These include F-Nβ species elongated by two and four amino acids (F-Nβ1733 and F-Nβ1735; Figure 4B). In addition, levels of F-Nβ terminating at amino acid 1734 (Figure 4B) were also slightly but reproducibly elevated (Figure 4A). Thus, inhibition of S3 cleavage by the PS1 L166P mutant does not cause a block of S4 cleavage, but rather shifts the

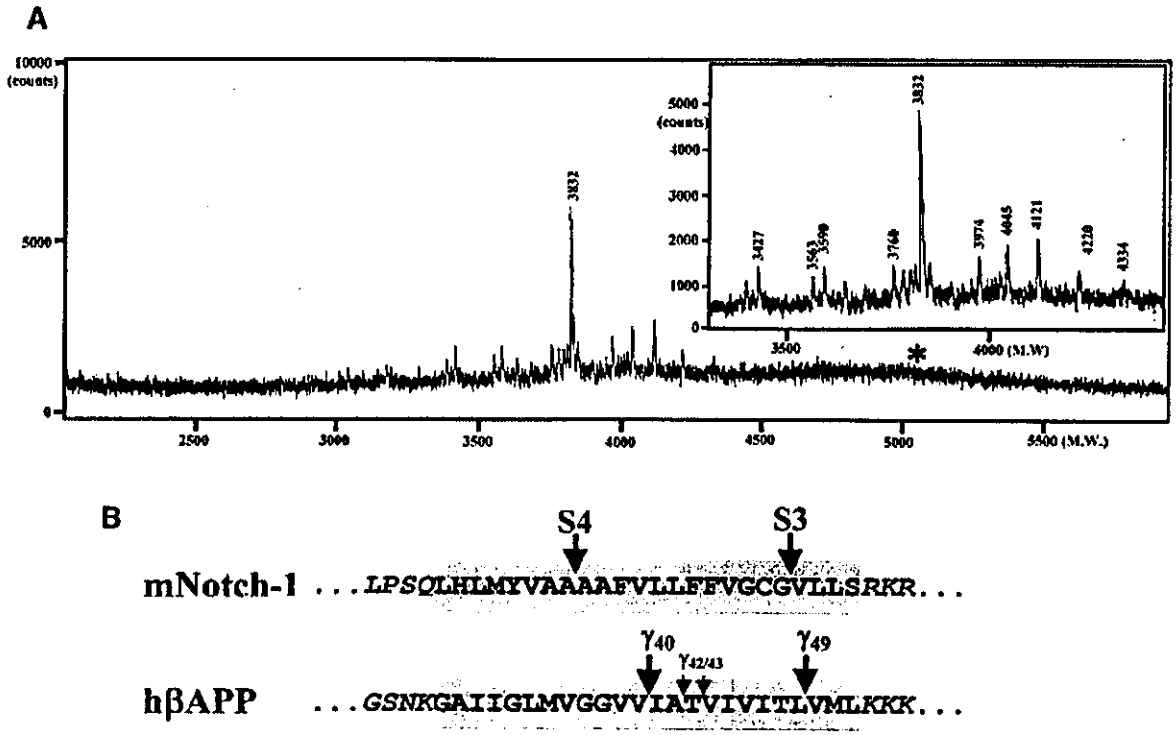

Fig. 2. Characterization of F-Nβ by IP/MS. (A) MALDI-TOF MS spectrum of F-Nβ. Conditioned medium from K293 cells stably expressing F-NEXT was immunoprecipitated with anti-FLAG M2 agarose, and F-Nβ was analyzed by MALDI-TOF MS (see Materials and methods). Molecular masses in Daltons of the individual peaks are indicated. Multiple peaks including a major peak at 3832 Da were observed at the mass range from 3400 to 4400 Da (inset). Peaks higher than 4400 Da including the theoretically predicted peak of ~5058 Da corresponding to F-Nβ derived from S3 cleavage (asterisk, see B) were not observed. The major F-Nβ peak of 3832 Da was also identified by IP/MS analysis from conditioned media of K293 cells stably transfected with F-NEXT M1727V (data not shown). (B) Schematic representation of intramembranous cleavages of the mouse Notch-1 and human βAPP TMs. S4 cleavage of F-NEXT derivatives occurs predominantly between Ala1731 and Ala1732.

Table I. List of F-Nβ species found in conditioned media

M_r (observed)	F-Nβ	M_r (calculated)	Amino acid sequence
4334	F-Nβ_{1736}	4333.81	LRDYKDDDDKMVMKSEPVEPPLPSQ LHLMYVAAAAFVL^{1736}
4220	F-Nβ_{1735}	4220.66	LRDYKDDDDKMVMKSEPVEPPLPSQ LHLMYVAAAAFV^{1735}
4121	F-Nβ_{1734}	4121.53	LRDYKDDDDKMVMKSEPVEPPLPSQ LHLMYVAAAAF^{1734}
3974	F-Nβ_{1733}	3974.36	LRDYKDDDDKMVMKSEPVEPPLPSQ LHLMYVAAAA^{1733}
4045	F-Nβ_{1731}	4045.45	RGLRDYKDDDDKMVMKSEPVEPPLPSQ LHLMYVAA^{1731}
3832	**F-Nβ_{1731}**	**3832.22**	**LRDYKDDDDKMVMKSEPVEPPLPSQ LHLMYVAA^{1731}**
3563	F-Nβ_{1731}	3562.89	DYKDDDDKMVMKSEPVEPPLPSQ LHLMYVAA^{1731}
3760	F-Nβ_{1730}	3761.15	LRDYKDDDDKMVMKSEPVEPPLPSQ LHLMYVA^{1730}
3590	F-Nβ_{1728}	3590.95	LRDYKDDDDKMVMKSEPVEPPLPSQ LHLMY^{1728}
3427	F-Nβ_{1727}	3427.78	LRDYKDDDDKMVMKSEPVEPPLPSQ LHLM^{1727}

Bold letters indicate a peptide sequence and its properties of the major species.

S4 cleavage in a manner similar to the effects caused by FAD mutant PS on γ_{40}/γ_{42} cleavage. Interestingly, the two other FAD mutants analyzed produced individual changes in C-terminal heterogeneity of the S4 cleavage. While PS1 C92S elevated levels of a peptide terminating after amino acid 1734, PS1 L286V increased peptides terminating after amino acid 1735 and decreased the levels of F-Nβ1734 (Figure 4A). Therefore, the FAD mutants analyzed apparently cause individual and characteristic cleavage patterns. They all have in common the increased production of elongated species. Like Aβ42 production, the levels of elongated F-Nβ are most affected significantly by the very aggressive PS1 L166P mutation, which causes FAD in early adulthood (Moehlmann *et al.*, 2002). These effects are not restricted to K293 cells, since we also observed similar effects of FAD-associated PS2 mutations in Neuro2a cells (data not shown). To substantiate these findings further, we performed multiple independent experiments followed by a semi-quantitative analysis (see Materials and methods). This fully confirmed the primary observations. All FAD mutants analyzed affected the generation of the F-Nβ C-terminus in a highly reproducible and quantitative manner (Figure 4C).

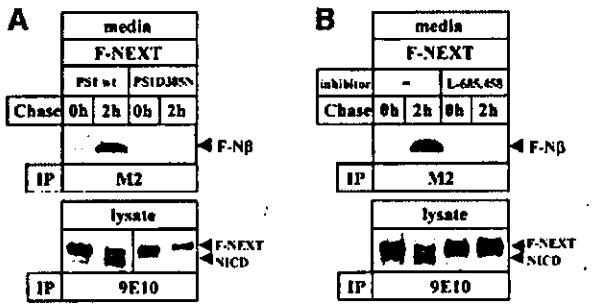

Fig. 3. F-Nβ is generated in a PS- and γ-secretase-dependent manner. (A) PS dependence of F-Nβ generation. K293 cells stably expressing wild-type PS1 or mutant PS1 D385N were stably transfected with the F-NEXT cDNA. Upper panel: F-Nβ generation was analyzed from conditioned media of metabolically labeled cells as described in Figure 1B. Lower panel: corresponding cell lysates were analyzed for NICD generation as described in Figure 1B. (B) γ-secretase dependence of F-Nβ generation. Upper panel: F-Nβ generation was analyzed as described in Figure 1B from conditioned media of K293 cells stably co-expressing F-NEXT and wild-type PS1 that were metabolically labeled in the presence or absence of γ-secretase inhibitor L-685,458 (1 μM). Lower panel: corresponding cell lysates were analyzed for NICD generation as described in Figure 1B.

Discussion

We have examined whether membrane-retained Notch fragments such as NEXT secrete peptides similar to Aβ upon NICD generation. Here we demonstrate that the NEXT derivative F-NEXT indeed undergoes an additional and unexpected cleavage at a novel site near the middle of the membrane, which results in the secretion of an Aβ-like peptide (Figure 5). Upon overexpression of F-NEXT, we identified several F-Nβ species with heterogeneous C-termini similar to Aβ. The major cleavage site was identified in the center of four sequential alanine residues between Ala1731 and Ala1732 in all cell lines analyzed so far (data herein and data not shown). Since it has been shown previously that NICD is generated by cleavage at S3 between Gly1743 and Val1744 (Schroeter *et al.*, 1998), one would have expected to detect a corresponding Nβ peptide terminating at Gly1743. However, in our study, we identified robust levels of peptides terminating at amino acid 1731, but failed to detect the secreted peptide corresponding to S3 cleavage in cultured media. Therefore, the intramembranous cleavage resulting in the immediate secretion of Nβ must be biochemically distinct from the previously identified S3 cleavage. Based on our findings, Nβ generation is therefore the result of a novel cleavage, and we consequently introduce the term S4 for this intramembranous cut.

Like AICD and Aβ production, generation of NICD and the novel Nβ are both dependent on PS-mediated γ-secretase processing. This is demonstrated by the significant reduction of Nβ generation upon the expression of a biologically inactive PS1 variant. Moreover, a highly potent γ-secretase inhibitor also blocked Nβ production. However, at present, we do not know the order of these cleavages. As discussed for AICD/Aβ generation (Sastre *et al.*, 2001), it is most likely that all the intramembranous γ-secretase cleavages occur simultaneously, since neither longer Aβ/Nβ nor AICD/NICD fragments have been identified so far.

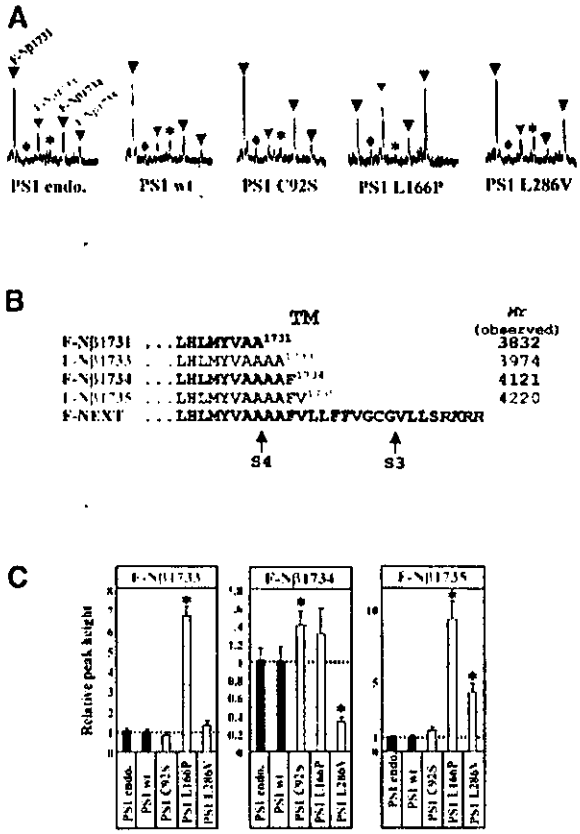

Fig. 4. PS1 FAD mutations affect the relative levels of elongated F-Nβ species. (A) MALDI-TOF MS spectra of F-Nβ species secreted from cells co-expressing F-NEXT and the indicated PS1 derivatives. Conditioned media were analyzed by IP/MS as described in Figure 2B. The mass range from ~3750 to ~4250 Da is shown. Black arrowhead, F-Nβ1731; colored arrowheads, F-Nβ1733 (green), F-Nβ1734 (blue) and F-Nβ1735 (red). The rhombus indicates the peak corresponding to F-Nβ1732 (molecular mass 3903 Da), and the asterisk indicates an F-Nβ1731 (molecular mass 4045 Da) species with a different N-terminus from that of the major F-Nβ1731 (molecular mass 3832 Da) species (compare Figure 2B and Table I). Note that FAD-associated PS1 mutations, in particular PS1 L166P, show an altered production of the various F-Nβ species. (B) C-termini of F-Nβ species affected by FAD-associated PS1 mutants. Sequences within the putative TM are shown. Black, F-Nβ1731; green, F-Nβ1733; blue, F-Nβ1734; red, F-Nβ1735. Arrows indicate S3 and S4. (C) Semi-quantitative analysis of elongated F-Nβ species. Conditioned media from cells expressing the indicated PS1 FAD-associated mutants (each medium amount for immunoprecipitation was normalized to contain the same level of F-Nβ1731; see Materials and methods) were analyzed by IP/MS. Peak heights corresponding to secreted F-Nβ1733, F-Nβ1734 and F-Nβ1735 were measured and are expressed relative to the peak height of the internal control (1 pmol bovine insulin β-chain; see Materials and methods). Asterisks indicate the significance of the increase and decrease of the various F-Nβ species relative to both endogenous/wild-type PS1-expressing cells ($P < 0.0001$; Students *t*-test). The data are the mean from five independent measurements.

Several PS-dependent γ-secretase substrates have been described. These include βAPP (De Strooper *et al.*, 1998), ErbB-4 (Ni *et al.*, 2001; Lee *et al.*, 2002), E-cadherin (Marambaud *et al.*, 2002), LRP (May *et al.*, 2002) and Notch-1–4 (De Strooper *et al.*, 1999; Mizutani *et al.*, 2001; Saxena *et al.*, 2001), and probably also CD44 (Okamoto *et al.*, 2001). Apparently, all these type I TM proteins release their C-terminal tails into the cytoplasm. Under

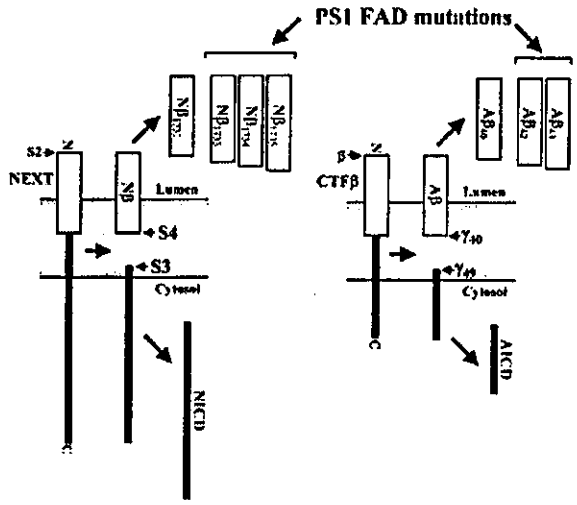

Fig. 5. Similar intramembranous cleavages of Notch-1 and βAPP. Following S2 cleavage, the Notch fragment NEXT is cleaved in a PS- and γ-secretase-dependent manner within the membrane at two major sites, S3 and S4. S3 cleavage occurs close to the cytosolic membrane border and leads to the liberation of NICD, whereas S4 cleavage occurs near the middle of the TM and causes the release of Nβ peptides. S3 and S4 cleavages are strikingly similar to γ_{49} and γ_{40} cleavages of CTFβ of βAPP, respectively. The generation of longer forms of Nβ and Aβ peptides ($A\beta_{42,43}$) are affected in a similar manner at least by some FAD-associated PS mutants.

in vivo conditions, some of the proteolytically liberated ICDs translocate to the nucleus (Schroeter *et al.*, 1998; Struhl and Adachi, 1998; Cao and Südhof, 2001; Ni *et al.*, 2001; Okamoto *et al.*, 2001; Lee *et al.*, 2002) where they do or may regulate transcription of target genes (reviewed in Steiner and Haass, 2001). The cleavage, which results in the liberation of ICDs, takes place very close to the cytoplasmic border of these proteins (Schroeter *et al.*, 1998; Gu *et al.*, 2001; Okamoto *et al.*, 2001; Sastre *et al.*, 2001; Yu *et al.*, 2001; Marambaud *et al.*, 2002; Weidemann *et al.*, 2002). In contrast, the γ-secretase cleavage of βAPP, which liberates Aβ, occurs in the middle of the TM. This apparent discrepancy has been used as an argument for the existence of two independent proteolytic enzymes involved in NICD generation and Aβ liberation (Yu *et al.*, 2001; reviewed in Sisodia and St George-Hyslop, 2002). Indeed, this idea may be supported by the selective inhibition of Aβ production without affecting Notch cleavage (Petit *et al.*, 2001). The consequence of these findings would be that Aβ generation and NICD (or even ICD production in general) is mediated by independent and distinct intramembrane cleaving proteases. However, our findings strongly support the idea that an evolutionarily conserved PS-dependent mechanism is involved in the two γ-secretase cleavages of Notch-1 and βAPP. Both result in the generation of the respective ICD (via cleavage close to the cytoplasmic border of the membrane) as well as the secretion of a small and hydrophobic peptide (via cleavage within the middle of the TM). The additional S4 intramembranous cleavage is also in agreement with recent findings demonstrating that an exchange of the βAPP TM with the Notch TM allows intramembranous γ-secretase processing at a position homologous to the site of Aβ40 generation (Zhang *et al.*, 2002). However, in the latter case, the cleavage was obtained several amino acids C-terminal of the S4 cleavage site determined in this study at a position corresponding to F-Nβ1735. The reason for this discrepancy is probably due to insertion of the Notch TM into an artificial βAPP backbone (Zhang *et al.*, 2002). In contrast, we used constitutively processed authentic Notch-1 derivatives mimicking NEXT. Finally, the selective inhibition of γ-secretase-mediated Aβ production (Petit *et al.*, 2001) has been challenged recently and it was clearly demonstrated that the inhibitors used do not directly affect PS-dependent γ-secretase cleavage and Aβ production (Esler *et al.*, 2002b).

Intramembranous endoproteolysis (S4/S3) of Notch-1 and βAPP shares many common features: (i) substrates of both S4/S3 and γ_{40}/γ_{49} cleavages are truncated extracellularly by shedding enzymes (reviewed in Mumm and Kopan, 2000; Steiner and Haass, 2000); (ii) S4/S3 (Figure 3) as well as γ_{40}/γ_{49} cleavages were found to be PS dependent; (iii) both the γ_{49} and S3 cleavages occur at analogous sites very close to the cytoplasmic border of the membrane (Schroeter *et al.*, 1998; Gu *et al.*, 2001; Sastre *et al.*, 2001; Yu *et al.*, 2001; Weidemann *et al.*, 2002); (iv) upon S4/S3 and γ_{40}/γ_{49} cleavages, the resulting fragments, Nβ/NICD (Figure 1) and Aβ/AICD, are released into the extracellular space or into the cytoplasm, respectively; (v) the extracellularly released fragments (Nβ/Aβ) do not correspond directly to the intracellularly released fragments (NICD/AICD), i.e. so far neither Nβ1743/Aβ49 nor NICD1732 (NICD starting from Ala1732, mouse Notch-1 numbering)/AICD59 (AICD starting from Ile41, Aβ numbering) have been identified; (vi) the C-termini of both peptides are heterogeneous; and, finally, (vii) FAD-associated mutants of PS1 cause the generation of C-terminally elongated Nβ fragments very similar to Aβ42 generated in the presence of FAD mutants (Figure 4). Due to these extensive similarities, it is very likely that the intramembraneous cleavages of both proteins occur by a common mechanism and are not mediated by different βAPP- and Notch-1-cleaving enzymes as proposed previously (Petit *et al.*, 2001, 2002a,b; Yu *et al.*, 2001; Taniguchi *et al.*, 2002; reviewed in Sisodia and St George-Hyslop, 2002). The conservation of this mechanism strongly suggests that at least Notch-1 and βAPP are cleaved twice by the same PS-dependent enzymatic mechanism. It certainly remains to be shown if the other γ-secretase substrates also undergo an additional intramembranous cleavage.

Finally, our data also support the hypothesis that PS harbors the catalytic site of γ-secretase and executes the cleavage of both βAPP and Notch-1. Interestingly, a very aggressive FAD-associated PS1 mutant (PS1 L166P), which causes an extreme increase of Aβ42 production, also dramatically shifts the corresponding cleavage of Notch-1. The most parsimonious explanation for this finding is a direct contact of PS with its substrates. Together with the finding that γ-secretase inhibitors bind to PS (Esler *et al.*, 2000; Li *et al.*, 2000), the observation of the 'critical aspartates' (Wolfe *et al.*, 1999), the similarity around the active site aspartate in TM7 of PSs to type 4 prepilin peptidases (Steiner *et al.*, 2000) and the finding